MCB Journals.ASM.org

Immunosuppression-Independent Role of Regulatory T Cells against Hypertension-Driven Renal Dysfunctions

Salvatore Fabbiano,[a,b] Mauricio Menacho-Márquez,[a,b] Javier Robles-Valero,[a,b] Miguel Pericacho,[c] Adela Matesanz-Marín,[d] Carmen García-Macías,[a,b] María A. Sevilla,[c] M. J. Montero,[c] Balbino Alarcón,[e] José M. López-Novoa,[c] Pilar Martín,[d] Xosé R. Bustelo[a,b]

Centro de Investigación del Cáncer[a] and Instituto de Biología Molecular y Celular del Cáncer,[b] Consejo Superior de Investigaciones Científicas (CSIC)-University of Salamanca, Salamanca, Spain; Departamento de Fisiología y Farmacología, University of Salamanca, Salamanca, Spain[c]; Centro Nacional de Investigaciones Cardiovasculares (CNIC), Madrid, Spain[d]; Centro de Biología Molecular Severo Ochoa, CSIC, Madrid, Spain[e]

Hypertension-associated cardiorenal diseases represent one of the heaviest burdens for current health systems. In addition to hemodynamic damage, recent results have revealed that hematopoietic cells contribute to the development of these diseases by generating proinflammatory and profibrotic environments in the heart and kidney. However, the cell subtypes involved remain poorly characterized. Here we report that CD39$^+$ regulatory T (T_{REG}) cells utilize an immunosuppression-independent mechanism to counteract renal and possibly cardiac damage during angiotensin II (AngII)-dependent hypertension. This mechanism relies on the direct apoptosis of tissue-resident neutrophils by the ecto-ATP diphosphohydrolase activity of CD39. In agreement with this, experimental and genetic alterations in T_{REG}/T_H cell ratios have a direct impact on tissue-resident neutrophil numbers, cardiomyocyte hypertrophy, cardiorenal fibrosis, and, to a lesser extent, arterial pressure elevation during AngII-driven hypertension. These results indicate that T_{REG} cells constitute a first protective barrier against hypertension-driven tissue fibrosis and, in addition, suggest new therapeutic avenues to prevent hypertension-linked cardiorenal diseases.

Foxp3$^+$ CD4$^+$ regulatory T (T_{REG}) cells are primarily involved in the negative control of conventional T-cell-dependent immune processes. To this end, they utilize a number of effector mechanisms, including cytokine-dependent paracrine signaling events, interleukin 2 consumption, presentation of immunosuppressive ligands, cytolysis of target cells, and modification of cell responses through the degradation of extracellular ATP. The latter regulatory mechanism is mediated by CD39, an ectoenzyme that displays ATP diphosphohydrolase activity (1, 2). In addition, T_{REG} cells can promote immunomodulation through the regulation of other hematopoietic cells, such as B lymphocytes, dendritic cells, and macrophages (1, 2). Recent observations have revealed that tissue-specific T_{REG} subtypes can also perform immunosuppression-independent functions. The best-characterized examples are the T_{REG} cells present in adipose tissue and injured skeletal muscles, which control metabolic indexes and muscle repair, respectively. These T_{REG} subsets are distinct from those involved in immunosuppression in terms of their T cell receptor repertoires and transcriptomal features (3, 4).

At present, hypertension and associated cardiovascular diseases represent one of the heaviest burdens for our health systems (5, 6). In addition to the hemodynamic damage inflicted by hypertension itself, a number of pathophysiological circuits that change the inflammatory, fibrotic, and functional status of peripheral tissues also influence the progression of these dysfunctions. If untreated, these processes eventually lead to end-organ disease and failure (7, 8). Extensive data indicate that T_{REG} cells play protective roles against high arterial pressure, cardiovascular remodeling, and heart damage (9–11). The exact nature of such protective action is unknown, although it has been commonly assumed that it is primarily associated with immunosuppression-linked mechanisms. In agreement with this, a large number of studies have shown that conventional T lymphocytes, the main cellular targets of T_{REG} cells, do play proactive roles during both the initiation and the progression of hypertension-related pathophysiological events (8, 12–22). The exact T cell subpopulation(s) involved in those processes is still under debate. Thus, some studies have proposed the involvement of different helper T (T_H17, T_H1, T_H2) subtypes in the engagement of these pathophysiological responses (13, 16, 17). In contrast, others have postulated that the extent of the hypertensive response is under the regulation of a nonconventional CD3$^+$ CD4$^-$ CD8$^-$ T cell subpopulation that is specifically localized in perivascular adipose tissue (15). These divergent results could reflect the involvement of different T cell subsets in tissue-specific pathophysiological responses of the vasculature, heart, and kidney. Settling this issue is of paramount importance for the design of new approaches to combat the inflammatory processes priming cardiorenal fibrosis and, eventually, end-organ disease. In the same context, it is important to clarify the specific role of T_{REG} cells in the regulation of this complex pathophysiological program and the cellular targets that they control.

The Vav family is a group of phosphorylation-dependent GDP/GTP exchange factors involved in the activation step of Rho proteins. This family has three members in mammalian species,

Received 19 May 2015 Returned for modification 19 June 2015
Accepted 24 July 2015
Accepted manuscript posted online 3 August 2015
Citation Fabbiano S, Menacho-Márquez M, Robles-Valero J, Pericacho M, Matesanz-Marín A, García-Macías C, Sevilla MA, Montero MJ, Alarcón B, López-Novoa JM, Martín P, Bustelo XR. 2015. Immunosuppression-independent role of regulatory T cells against hypertension-driven renal dysfunctions. Mol Cell Biol 35:3528–3546. doi:10.1128/MCB.00518-15.
Address correspondence to Xosé R. Bustelo, xbustelo@usal.es.

doi:10.1128/MCB.00518-15

designated Vav1 (formerly known as Vav, or p95^{vav}), Vav2, and Vav3. Vav1 is expressed primarily in most hematopoietic lineages, whereas Vav2 and Vav3 show more-widespread expression patterns (23–25). Vav1 and, to a lesser extent, the other Vav family members are important for lymphocyte development, selection, and effector functions (23–25). In agreement with this, single-knockout (*Vav1*$^{-/-}$) and triple-knockout (*Vav1*$^{-/-}$; *Vav2*$^{-/-}$; *Vav3*$^{-/-}$) (*TKO*) mice exhibit both peripheral T cell lymphopenia and deficient, T cell receptor-dependent antigenic responses (26–28). Vav2 and Vav3, but not Vav1, are also involved in signaling routes contributing to cardiovascular homeostasis. As a consequence, the elimination of one or both of these proteins causes hypertension, cardiovascular remodeling, cardiorenal fibrosis, and renal dysfunctions in mice (29–32). Based on these observations, we believed that this collection of Vav family knockout mice could represent a useful tool for clarifying obscure aspects of the interplay between the immune and cardiovascular systems during hypertension. The use of these animals, together with other experimental mouse models of immunodeficiency and hypertension, allowed us to discover a hitherto unknown T_{REG} cell-dependent mechanism that controls the extent of the overall arterial pressure response and end-organ dysfunctions under angiotensin II (AngII)-dependent hypertension conditions. As we show here, this mechanism is unexpectedly mediated by the direct, CD39- and apoptosis-mediated homeostatic control of tissue-resident neutrophil numbers rather than by standard T cell immunosuppression processes. Hence, it is fully operative even in the complete absence of conventional T lymphocytes. This new mechanism offers potentially interesting therapeutic avenues for preventing cardiorenal fibrosis and the ensuing end-organ disease in patients with long-term, AngII-dependent types of hypertension.

MATERIALS AND METHODS

Animals. *Vav1*$^{-/-}$ and *Vav2*$^{-/-}$; *Vav3*$^{-/-}$ mice have been described previously (27, 29, 30). All *Vav* family knockout mice were homogenized in the C57BL/10 genetic background. *Ly5.1*$^{+}$ mice were originally obtained from The Jackson Laboratories and were maintained at the animal facility of the Centro de Biología Molecular Severo Ochoa (CSIC, Madrid, Spain). For the experiments, animals were transferred to the animal facility of the Centro de Investigación del Cáncer. BALB/c, SCID (severe combined immunodeficiency)/beige (C.B-17/lcrHsd-*Prkdc*^{scid}*Lyst*$^{bg\text{-}J}$), and *Foxn1*^{nu} mice were obtained from Harlan Laboratories. For all *in vivo* studies, animals of the same genotype were randomly assigned to the different experimental groups. The animals used were either 4 months old (for analysis of basal conditions) or 3 months old (for analyses using osmotic pumps). All animal work has been done in accordance with protocols approved by the Bioethics committees of the University of Salamanca, the CSIC, and the Centro Nacional de Investigaciones Cardiovasculares.

Blood pressure-related analyses. Mean blood pressure was recorded for conscious mice by the noninvasive tail cuff method (Coda system; Kent Scientific). Mice were familiarized with the procedure during the week prior to data recording in order to minimize stress-related blood pressure variations. Blood pressure measurements were always taken in the afternoon.

Histological analyses. Tissues were fixed in 4% paraformaldehyde in a phosphate-buffered saline solution, embedded in paraffin, cut into 2- to 3-μm sections, and stained with hematoxylin and eosin (H&E) (Sigma). Aorta media walls and cardiomyocyte areas were quantified with MetaMorph software (Universal Imaging).

Tissue fibrosis determinations. Fibrosis was quantified both immunohistochemically and biochemically. In the former case, paraffin-embedded tissue sections were stained with Sirius red (Fluka). In the latter case, we measured the amount of hydroxyproline present in tissue lysates. Data from those analyses were converted into amounts of collagen by considering that collagen contains 12.7% hydroxyproline residues. These two procedures were carried out as described previously (29, 30).

Analysis of kidney function. Mice were placed in metabolic cages, and daily urine production was collected and measured, as described previously (30). The protein content in the urine was detected with the Bradford protein assay reagent (Bio-Rad) by using a standard curve of bovine serum albumin (Sigma). To calculate creatinine clearance rates, we collected urine from individual mice over a 24-h period by using metabolic cages. In addition, we took blood samples from the animals under study by cardiac puncture in order to measure the concentration of creatinine in plasma. Concentrations of creatinine in urine and plasma were determined by a kinetic colorimetric method using a creatinine assay kit (QuantiChrom creatinine assay kit; BioAssay Systems) according to the manufacturer's protocol. The creatinine clearance rate (CCR) was calculated by taking into account the urine flow (uf) and the concentrations of creatinine in both urine ([Cre]u) and plasma ([Cre]p), using the formula CCR = uf × [Cre]u/[Cre]p. Values were further normalized by taking the weight of kidneys into account.

Determination of mRNA abundance. RNA was extracted with TRIzol (Sigma), and quantitative reverse transcription-PCR (RT-PCR) was performed with a Script one-step RT-PCR kit (Bio-Rad) on a StepOnePlus real-time PCR system (Applied Biosystems). Data were analyzed with StepOne software, version 2.1 (Applied Biosystems). Expression of the endogenous mouse *P36b4* transcript was used as a normalization control. The primers used were 5′-TTG ATG ATG GAG TGT GGC ACC-3′ (forward) and 5′-GTG TTT GAC AAC GGC AGC ATT-3′ (reverse) for mouse *P36b4* cDNA and 5′-CAC CAC GGA CTA CAA CCA GTT CGC-3′ (forward) and 5′-TCA GTT GTC AAT GCA TTG GTC GGT G-3′ (reverse) for mouse *Lcn2* cDNA.

Pharmacological treatments of mice. AngII (1.44 mg/kg of body weight/day; Sigma) and ARL 67156 (1.1 μg/kg/day; Sigma) were administered for 14 days using osmotic delivery pumps (model 1002; Alzet) inserted subcutaneously into the backs of animals. N_{ω}-nitro-L-arginine methyl ester (L-NAME) (70 mg/100 ml; Sigma) was administered in the drinking water for 4 weeks (32). Mycophenolate mofetil (MMF) (CellCept; Roche Farma) was prepared as described previously (33) and was administered as described below.

Isolation of hematopoietic cells from tissues. For the isolation of kidney-infiltrating cells, anesthetized mice were infused with a phosphate-buffered saline solution through the left ventricle of the heart to eliminate kidney-resident circulating cells. The two kidneys of each mouse were then collected, decapsulated, cut into small pieces with a sterile scalpel, and incubated in 10 ml of RPMI medium containing 10% fetal bovine serum and collagenase (5 mg; Sigma) for 20 min at 37°C. After the filtering of tissue debris, cells were washed twice with a phosphate-buffered saline solution and were resuspended in 8 ml of RPMI medium plus 10% fetal bovine serum. Upon the addition of a 5-ml lower layer of Ficoll (Sigma) with a pipette, samples were centrifuged at 2,000 rpm at room temperature for 10 min. Cells at the medium-Ficoll interface were collected using a pipette and were counted. To obtain cells from the spleen and thymus, single-cell suspensions were obtained by mechanical homogenization of tissues in 1 ml of a phosphate-buffered saline solution supplemented with 2% bovine serum albumin and 0.5 mM EDTA. Bone marrow neutrophils were obtained by flushing the medullar cavities of isolated femoral bones with a phosphate-buffered saline solution. To obtain circulating cells, blood samples were collected from hearts by use of heparinized syringes. The cell suspensions obtained under the conditions described above were washed once in a phosphate-buffered saline solution, subjected to lysis with 0.17 M NH_4Cl to eliminate erythrocytes, and finally washed twice. The final cell pellets were resuspended in a phosphate-buffered saline solution before the immunostaining step.

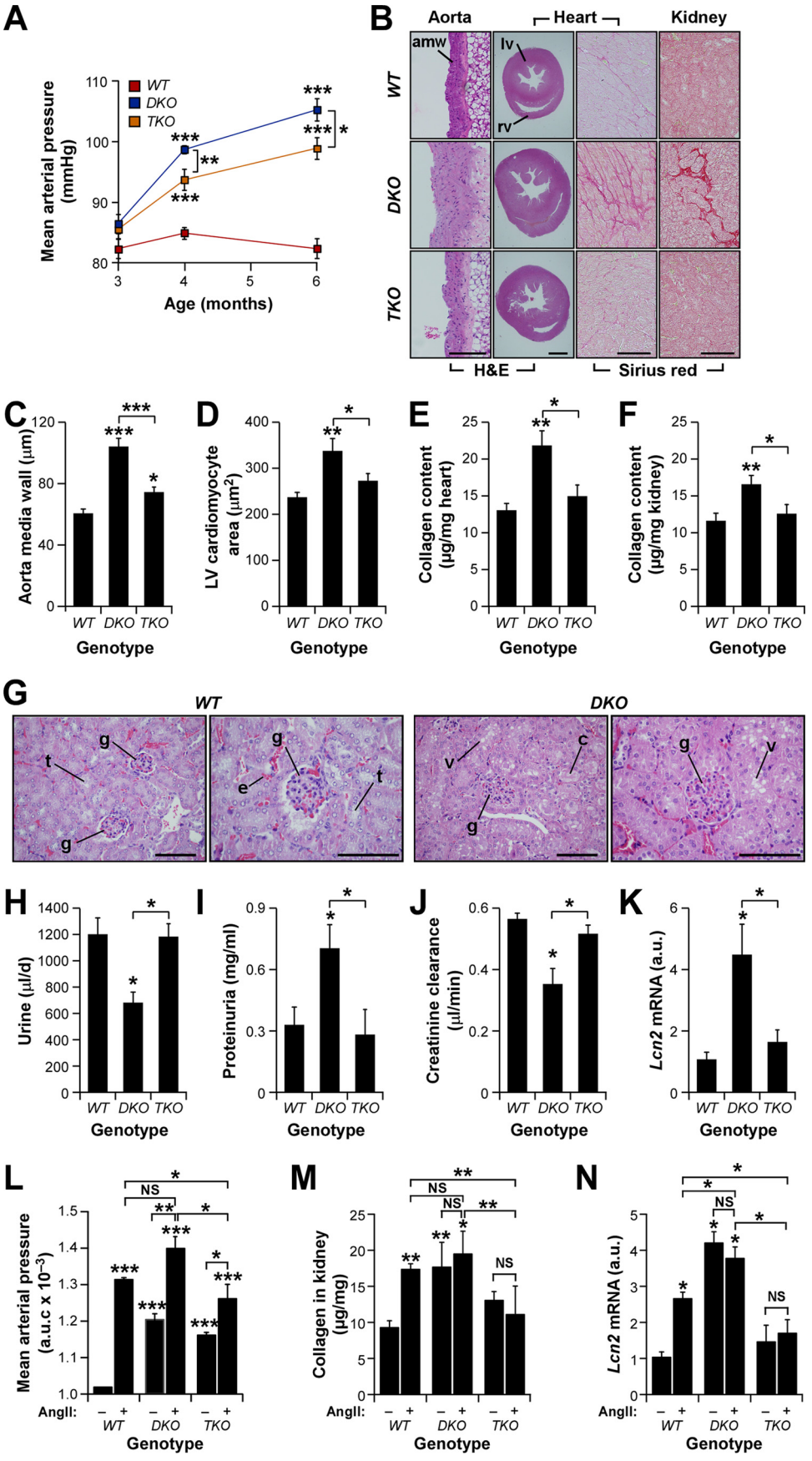

Characterization and isolation of hematopoietic cells. The cell suspensions obtained as described above were stained with combinations of fluorescein isothiocyanate (FITC)-, allophycocyanin (APC)-, APC-Cy7-, or V500-labeled antibodies to CD4 (BD Biosciences), FITC-, Pacific Blue (PB)-, or phycoerythrin (PE)-labeled antibodies to CD8 (BD Biosciences), APC- or PE-Cy7-labeled antibodies to CD25 (BD Biosciences), FITC- or APC-labeled antibodies to Gr1 (eBioscience or BD Biosciences, respectively), APC- or PE-Cy7-labeled antibodies to F4/80 (eBioscience or BD Biosciences, respectively), PE-labeled antibodies to CD11b (BD Biosciences), PE- or FITC-labeled antibodies to CD11c (BD Biosciences), biotin- or APC-labeled antibodies to B220 (BD Biosciences), or PE-Cy7-labeled anti-CD39 (eBioscience). Cell immunolabeling with either FITC- or PE-labeled antibodies to Foxp3 was carried out using the Foxp3 staining buffer set (eBioscience). For data acquisition, samples were collected using a FACSAria III flow cytometer (BD Biosciences) and were blindly analyzed using FlowJo software (Tree Star). For *in vitro* studies, samples were sorted under sterile conditions using a FACSAria III system, collected in a phosphate-buffered saline solution supplemented with 50% fetal bovine serum, centrifuged, resuspended in RPMI medium (Gibco Life Technologies) supplemented with 10% fetal bovine serum, 2 mM L-glutamine, and antibiotics (100 U/ml penicillin and 100 μg/ml streptomycin; Invitrogen) (referred to below as complete medium), and cultured in complete RPMI medium as indicated.

Generation of iT_{REG} cells. Freshly sorted splenic $CD4^+$ $CD25^-$ T cells were plated (1×10^6 cells/ml) onto culture dishes coated with antibodies to mouse CD3 (5 μg/ml; BD Biosciences) and containing complete RPMI medium supplemented with antibodies to CD28 (5 μg/ml; BD Biosciences), transforming growth factor β_1 (5 ng/ml; R&D Systems), and recombinant mouse interleukin 2 (100 IU/ml; Peprotech). The cells were then cultured for 4 days, centrifuged, washed twice with a phosphate-buffered saline solution, and stained with FITC-labeled anti-CD4 (BD Biosciences), APC-labeled anti-CD25 (BD Biosciences), and PE-Cy7-labeled anti-CD39. The induced T_{REG} (iT_{REG}) cell population was either separated as a whole $CD4^+$ $CD25^+$ population or fractionated into $CD4^+$ $CD25^+$ $CD39^+$ and $CD4^+$ $CD25^+$ $CD39^-$ populations before being injected into animals. Cells were collected for *in vivo* experiments using a FACSAria cell sorter as described above.

Injection of T_{REG} cells into mice. iT_{REG} cells generated as described above and freshly sorted splenic $CD4^+$ $CD25^+$ natural T_{REG} (nT_{REG}) cells were resuspended in 100 μl of a phosphate-buffered saline solution at a density of 2×10^6 cells/ml and were injected into the lateral tail vein 1 day after the implantation of the drug delivery pumps. Unless otherwise stated, 2×10^5 cells were injected per animal in these experiments. Where indicated, injections were performed with spleen-derived $CD4^+$ $CD25^-$ T cells as described above.

Immunodepletion of nT_{REG} cells. Two hundred fifty micrograms of either a monoclonal rat antibody to mouse CD25 (clone PC61.5; eBioscience) or an IgG1(κ) isotype negative control (eBioscience) was injected intraperitoneally 1 day before the implantation of drug delivery osmotic pumps. The extent of immunodepletion achieved in each animal was assessed weekly by flow cytometry. To that end, blood was drawn from anesthetized mice, and cells were collected, washed in a phosphate-buffered saline solution, subjected to 0.17 M NH_4Cl-mediated erythrocyte lysis, washed twice with a phosphate-buffered saline solution, stained with both FITC-labeled CD4 and APC-labeled CD25, and analyzed by flow cytometry.

Immunodepletion of neutrophils. Wild-type (*WT*) mice were injected intraperitoneally with either 500 μg of a rat monoclonal antibody to the Ly6G surface marker (clone 1A8; Biolegend) or the same amount of an IgG1(κ) isotype negative control (eBioscience) 1 day before the implantation of osmotic pumps for AngII delivery. The percentages of neutrophils in blood were assessed every 3 days by flow cytometry using FITC-labeled antibodies to Gr1. At the end of the experiments, the percentages of neutrophils, macrophages, and $CD4^+$ T cells in kidneys were determined by labeling cells with antibodies to Gr1 (FITC labeled; eBiosciences), CD11b (PE labeled; BD Biosciences), F4/80 (APC labeled; BD Biosciences), and CD4 (V500 labeled; BD Biosciences).

Neutrophil recruitment assays. Where indicated, conditioned cell culture supernatants were obtained from fresh cultures of splenic T cells (see Fig. 8) at 1×10^6 cells/ml. After 72 h, the cells were centrifuged and supernatants collected. For chemotactic assays, 1×10^5 freshly purified bone marrow neutrophils were placed in the upper chamber of a Transwell plate (Corning HTS 24-well Transwell; pore size, 3.0 μm) that contained, in the lower chamber, complete RPMI medium, cell-conditioned supernatants from the cell types indicated in Fig. 8, and, where indicated, complete RPMI medium supplemented with 1 μM angiotensin II.

Determination of ROS production and apoptosis in neutrophil cultures. Freshly sorted bone marrow neutrophils were cultured in complete RPMI medium and were treated with 1 μM AngII II for 20 min. Where indicated, cells were pretreated with either 10 μM losartan (Merck) or 10 μM PD123319 (Sigma) for 30 min. A 10 μM concentration of MMF (Roche Farma) was included in cultures for 120 min before the angiotensin II stimulation. For neutrophil–nT_{REG} cell coculture experiments, cells were sorted as described above, either left untreated or treated with 250 μM ARL 67156 in complete RMPI medium for 30 min, and then cultured together in the same culture medium for 24 h, always using an nT_{REG} cell-to-neutrophil ratio of 1:10. In some of these experiments, nT_{REG} cells were either replaced or cocultured with other T cells, and the same experimental procedure was followed. Reactive oxygen species (ROS) production and apoptosis by neutrophils were assessed using lucigenin-based chemiluminescence (34) and annexin V/propidium iodide flow cytometry determinations (35), respectively. The latter assay was carried out using the Apoptosis Detection kit from Immunostep.

Statistics. Data were analyzed by either a two-tailed Student *t* test or one-way analysis of variance (ANOVA) with a Bonferroni *post hoc* test in the case of multiple comparisons.

RESULTS

Vav proteins are important for hypertension-driven cardiorenal fibrosis. We have reported before that *Vav2*$^{-/-}$, *Vav3*$^{-/-}$, and

FIG 1 Vav family *TKO* mice show protection against heart hypertrophy and cardiorenal fibrosis. (A) Evolution of mean arterial pressure in mice of the indicated genotypes. *, $P \leq 0.05$; ***, $P \leq 0.001$ ($n = 8$). (B) Examples of aorta, heart ventricle, left ventricle, and kidney sections (from left to right) obtained from 4-month-old mice of the indicated genotypes. Sections were stained as indicated. Sirius red-stained fibrotic deposits in interstitial areas are seen as dark pink areas (right). amw, aorta media wall; lv, left ventricle; rv, right ventricle. Bars, 100 μm. Similar results were obtained using serial sections and independent mice ($n = 4$). (C to F) Status of cardiovascular (C and D) and cardiorenal (E and F) parameters in mice of the indicated genotypes. LV, left ventricle. Asterisks indicate significant differences (*, $P \leq 0.05$; **, $P \leq 0.01$; ***, $P \leq 0.001$) from the control or between the experimental groups indicated ($n = 4$). (G) Examples of kidney sections from mice of the indicated genotypes. *WT* mice exhibit normal glomeruli (g) and tubules (t), whereas *DKO* animals display typical signs of glomerular sclerosis, cytoplasmic vacuolar accumulation (v) in necrotic tubules, and protein casts (c). Erythrocytes (e) are seen as red spots in all sections. Bars, 50 μm. (H to J) Daily urine production ($n = 6$) (H), urine protein content ($n = 6$) (I), and creatinine clearance rates ($n = 4$) (J) in mice of the indicated genotypes. An asterisk indicates a significant difference ($P \leq 0.05$) from the control or between the experimental groups indicated. (K) Levels of *Lcn2* transcripts in the kidneys of animals of the indicated genotypes. An asterisk indicates a significant difference (*, $P \leq 0.05$) from the control or between the experimental groups indicated ($n = 4$). (L to N) AUC (area under the curve) for mean arterial pressure (L) and renal parameters (M and N) in mice of the indicated genotypes that had either been left untreated (−) or infused with AngII (+). Asterisks indicate significant differences (*, $P \leq 0.05$; **, $P \leq 0.01$; ***, $P \leq 0.001$) from the control or between the experimental groups indicated ($n = 4$). NS, not statistically significant. Error bars in all figures represent the standard errors of the means.

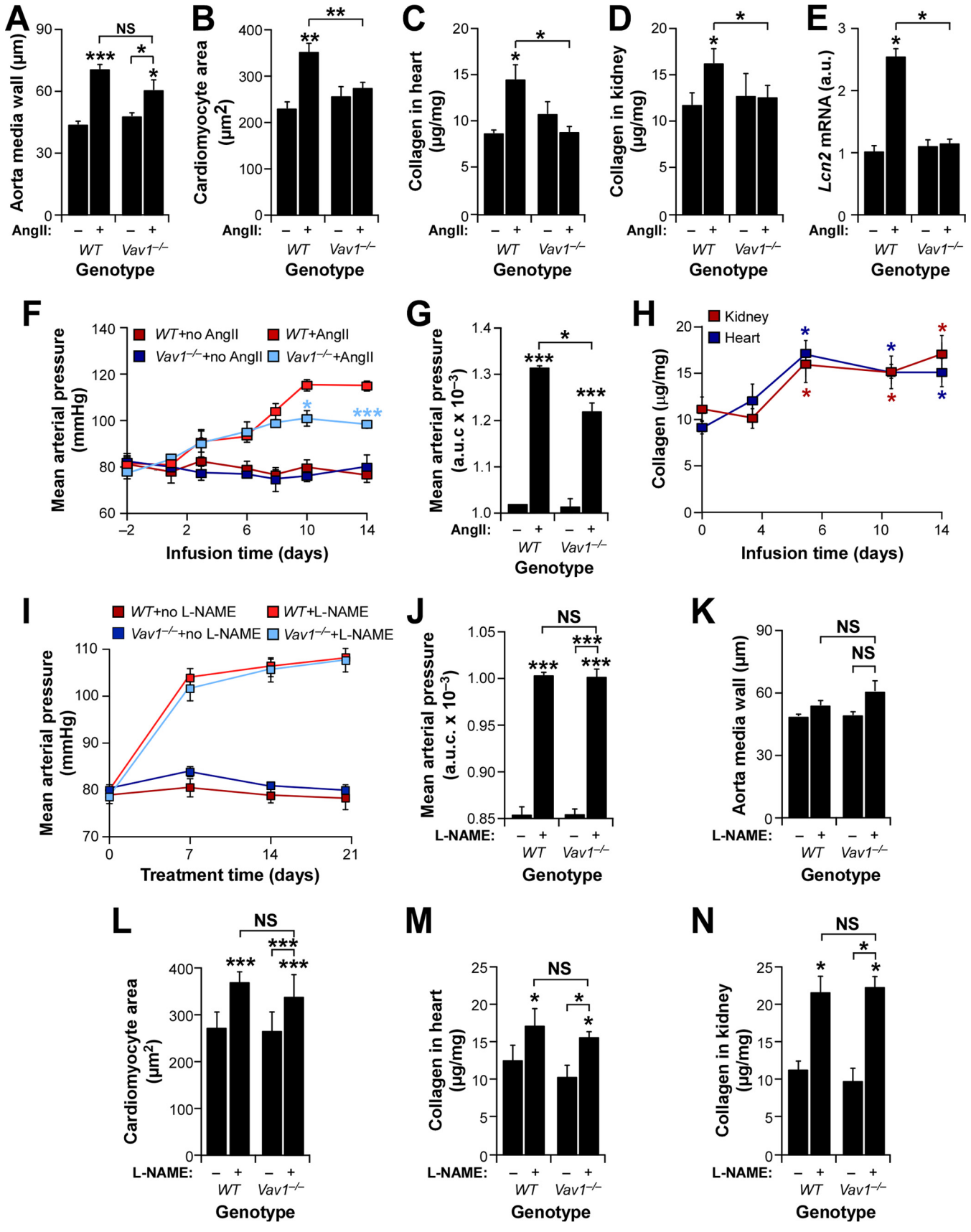

Vav2$^{-/-}$; *Vav3*$^{-/-}$ (double knockout [*DKO*]) mice develop hypertension in an age- and AngII-dependent manner (Fig. 1A) (29, 30, 32). Further analyses indicated that *DKO* mice also develop hypertension-linked dysfunctions similar to those present in the *Vav2*$^{-/-}$ and *Vav3*$^{-/-}$ single-knockout animals, including thickening of the aorta media wall (Fig. 1B, left panels, and C), hypertrophy of left ventricle cardiomyocytes (Fig. 1B, second panels from left, and D), and interstitial fibrosis in both the heart (Fig. 1B, second panels from right, and E) and the kidney (Fig. 1B, right panels, and F). Signs of the latter condition included the detection of collagen by Sirius red staining (Fig. 1B, two rightmost panels) and hydroxyproline tissue content (Fig. 1E and F) in both heart and kidney tissue samples. Furthermore, the histological analyses of kidneys revealed the presence of extensive glomerular sclerosis, necrosis of distal tubules, and protein casts in kidney sections from *DKO* mice (Fig. 1G). In agreement with this, we observed that *DKO* mice also exhibit alterations in renal physiology, such as reduced urine flow (Fig. 1H), increased protein content in urine (proteinuria) (Fig. 1I), reduced creatinine clearance rates (Fig. 1J), and increased amounts of the lipocalin 2 (Lcn2) transcript (Fig. 1K), a well-known early biomarker for both acute and chronic nephropathies (36). These results led us to investigate the effect of the additional inactivation of the *Vav1* gene in this cardiovascular phenotype using the *Vav1*$^{-/-}$; *Vav2*$^{-/-}$; *Vav3*$^{-/-}$ triple-knockout (*TKO*) mouse strain. We found that these mice exhibit hypertension (Fig. 1A) and vascular remodeling (Fig. 1B, left, and C), although at levels statistically significantly lower than those in *DKO* mice (Fig. 1A and C). However, we found, unexpectedly, that *TKO* mice show no obvious signs of cardiomyocyte hypertrophy (Fig. 1B, second panels from left, and D) or cardiorenal fibrosis (Fig. 1B, rightmost panels, E, and F). They also show normal urine production rates (Fig. 1H), urine protein content (Fig. 1I), creatinine clearance (Fig. 1J), and intrarenal *Lcn2* transcript amounts (Fig. 1K), further indicating that these mice have no significant signs of heart remodeling or of cardiorenal fibrosis in the kidneys.

We surmised that the mild hypertension present in *TKO* mice could be the cause of the protection exhibited by these animals against cardiorenal fibrosis and cardiovascular remodeling. To explore this possibility, we decided to compare the pathophysiological parameters mentioned above in wild-type (*WT*), *DKO*, and *TKO* mice under conditions of systemic administration of AngII, a well-known vasoconstriction agent (37). We speculated that if the idea presented above was correct, then chronic delivery of this vasoconstriction agent had to restore cardiorenal fibrosis and heart remodeling in *TKO* mice. To this end, we implanted AngII delivery osmotic pumps in the backs of *WT*, *DKO*, and *TKO* animals and subsequently followed the evolution of blood pressure over a 14-day period. In addition, we monitored the rest of the cardiovascular and renal parameters using samples from mice euthanized at the end of AngII treatment. As expected, such conditions promote the development of high blood pressure (Fig. 1L), renal fibrosis (Fig. 1M), and increased levels of *Lcn2* transcripts in kidneys (Fig. 1N) in *WT* mice. Likewise, they exacerbate the hypertensive state of *DKO* mice (Fig. 1L). However, this change in arterial blood pressure does not lead to further increases in the already high levels of collagen deposition (Fig. 1M) and *Lcn2* mRNA expression (Fig. 1N) in the kidneys of *DKO* mice. Systemic infusion of AngII also aggravates the hypertensive state of *TKO* mice, though to a lower extent than those for AngII-infused *DKO* and *WT* mice (Fig. 1L). However, under these conditions, arterial blood pressure does reach levels comparable to those exhibited by untreated *DKO* mice (Fig. 1L), which, as shown above, do develop cardiorenal fibrosis (Fig. 1C to K). Despite this, AngII-treated *TKO* mice still show no change in renal fibrosis-related parameters (Fig. 1M and N). These results suggest that the differences in overall arterial blood pressure could not be the main cause of the different cardiorenal phenotypes exhibited by *DKO* and *TKO* mice. In addition, the results indicate that Vav proteins play either direct or indirect roles in hypertension-driven cardiorenal fibrosis.

***Vav1* gene deficiency is sufficient to confer protection against tissue fibrosis.** To investigate whether the protection exhibited by *TKO* mice against heart remodeling and cardiorenal fibrosis was due to the elimination of the three *Vav* family genes or to the single inactivation of the *Vav1* gene, we next compared the responses of control and *Vav1*$^{-/-}$ single-knockout mice to systemic administration of AngII. Except for the normal development of vascular remodeling (Fig. 2A), AngII-infused *Vav1*$^{-/-}$ mice develop no obvious signs of cardiomyocyte hypertrophy (Fig. 2B), cardiorenal fibrosis (Fig. 2C and D), or changes in the expression of *Lcn2* mRNA in the kidneys (Fig. 2E). Furthermore, although AngII-infused *Vav1*$^{-/-}$ mice initially show elevations in blood pressure similar to those of controls (Fig. 2F), they eventually exhibit less-severe hypertension than *WT* animals at later periods during systemic administration of AngII (Fig. 2F and G). The differential response takes place between the 6th and the 10th day of AngII infusion, roughly corresponding to the time in which cardiorenal fibrosis reaches a plateau in control mice (Fig. 2H). Thus, the elimination of the *Vav1* gene fully recapitulates the effects of the removal of the three Vav family members in this pathophysiological scenario. In contrast to the findings for AngII-driven hypertension, we observed that *Vav1*$^{-/-}$ mice are not protected against the dysfunctions under study when treated with the nitric oxide synthase inhibitor Lω-nitro-L-arginine methyl ester (L-NAME) (Fig. 2I to N). This compound promotes hypertension through the blockage of the nitric oxide-mediated dilatation of resistance blood vessels (38). These results suggest that the antifibrotic protection induced by the *Vav1* gene deficiency probably is not due to a nonspecific, buffering effect on the damaging hemodynamic effects of hypertension on peripheral tissues.

Immunosuppressed mice show no resistance to hypertension-linked tissue fibrosis. *Vav1*$^{-/-}$ and *TKO* mice, unlike *DKO*

FIG 2 *Vav1* gene deficiency protects against AngII-triggered cardiorenal dysfunctions. (A to E) Status of the indicated cardiovascular (A to C) and renal (D and E) parameters in mice of the indicated genotypes infused with AngII (+) or left untreated (−). *, $P \leq 0.05$; **, $P \leq 0.01$; ***, $P \leq 0.001$ ($n = 10$). a.u., arbitrary units. (F and G) Mean arterial pressure evolution (F) and area under the curve (AUC) (G) for the indicated mouse strains and treatments. *, $P \leq 0.05$; ***, $P \leq 0.001$ ($n = 6$). (H) Kinetics of cardiorenal fibrosis development in AngII-treated *WT* mice. *, $P \leq 0.05$ ($n = 4$). (I and J) Evolution (I) and AUC (J) of mean arterial pressure in mice of the indicated genotypes in the presence or absence of L-NAME. ***, $P \leq 0.001$ ($n = 4$). (K to N) Status of the indicated vascular (K), heart (L and M), and renal (N) parameters in *WT* and *Vav1*$^{-/-}$ mice at the end of L-NAME treatment. Note that, in contrast to AngII infusion, oral administration of L-NAME does not induce aorta remodeling even in *WT* mice (K). *, $P \leq 0.05$; ***, $P \leq 0.001$ ($n = 4$). Statistical differences from untreated *WT* controls or between the indicated experimental groups are indicated.

animals, have reduced numbers of peripheral T cells, which, in addition, cannot adequately respond to antigens (26–28). Based on previous reports indicating that conventional T cells are implicated in the development of hypertension, tissue fibrosis, and end-organ disease (7, 8, 12, 13, 20), we surmised that the lymphopenic status of these two mouse strains could be the main cause of the resistance shown to AngII-triggered heart remodeling and cardiorenal fibrosis. We assumed that if that was the case, a similar phenotype had to be found in other immunocompromised mice. In agreement with this idea and with published results (12, 13), we initially found that treatment of AngII-infused *WT* mice with the T cell immunosuppressant mycophenolate mofetil (MMF) (39) does lead to a hypertensive buffering effect and protection against cardiorenal fibrosis (S. Fabbiano, unpublished data). As an additional control to corroborate these results, we next decided to analyze the response of mice of the *Foxn1*^{nu} strain, which cannot generate T lymphocytes due to problems in the development of the thymus, to AngII infusion. Unexpectedly, in this case, we found no significant protection against cardiorenal fibrosis (Fig. 3A and B) and a total lack of the hypertension buffering effect (Fig. 3C) that had been seen in *Vav1*$^{-/-}$ mice. Similar results were obtained with AngII-treated SCID (severe combined immunodeficiency)/beige mice, which lack both T and B lymphocytes (Fabbiano, unpublished; see also Fig. 7). We inferred from these experiments that T cell immunosuppression *per se* cannot explain the results obtained with *Vav1*$^{-/-}$ and MMF-treated *WT* mice and that therefore, other cell types had to be involved in the development of cardiorenal fibrosis during AngII-triggered hypertension. In agreement with this idea, we found that MMF also promotes resistance to both cardiorenal fibrosis (Fig. 3A and B) and excessive elevations of blood pressure (Fig. 3C) when administered to AngII-infused *Foxn1*^{nu} mice.

Taking into account the fact that the *Vav1* gene is expressed predominantly in hematopoietic cells (23), we hypothesized that alterations in cells belonging to either the adaptive or the innate immune system had to be involved in the protection against fibrosis exhibited by *Vav1*$^{-/-}$ mice. As a first step in identifying these cells, we carried out flow cytometry determinations to analyze the distribution of a large variety of hematopoietic cell lineages in kidneys, blood, spleens, and thymi from *DKO* mice (which showed no cardiorenal protection), *TKO* mice (which exhibited cardiorenal protection), *Vav1*$^{-/-}$ mice (normotensive and immunodeficient), and normotensive *WT* mice. We excluded the heart from these studies due to the difficulty of avoiding cross-contamination from the large numbers of circulating cells present in that tissue. We found that *TKO* and *Vav1*$^{-/-}$ mice have lower numbers of both neutrophils and CD4$^+$ cells in their kidneys than the other mouse strains (Table 1). This neutropenia is kidney specific; no statistically significant differences in circulating neutrophils are detected between *TKO* and *DKO* mice (Table 1). However, these two mouse knockout strains do exhibit neutrophilia in the blood relative to neutrophil levels in *WT* and *Vav1*$^{-/-}$ animals (Table 1). Whether this is due to their common hypertensive condition remains unknown. In contrast to the pattern of neutrophils, the CD4$^+$ T cell lymphopenia found in the kidneys of *TKO* and *Vav1*$^{-/-}$ mice is also seen in the rest of the tissues surveyed (Table 1), a result consistent with the known intrathymic T cell selection defects in those mice (27). Unexpectedly, further flow cytometry analyses revealed that the CD4$^+$ T cell lymphopenia of *TKO* and *Vav1*$^{-/-}$ mice does not apply to CD4$^+$ Foxp3$^+$ T_{REG} cells; the percentages of these immunoregulatory cells in all tissues surveyed in these mice are comparable to those for *WT* and *DKO* animals (Table 1). We observed no statistically significant differences in the percentages of other hematopoietic lineages surveyed, including macrophages, CD11c$^+$ and CD11c$^-$ dendritic cells, CD8$^+$ T cells, and B lymphocytes, in the kidneys of control, *DKO*, *TKO*, and *Vav1*$^{-/-}$ mice (Table 1). These results suggested that either T_{REG} cells, neutrophils, or both cell lineages combined could be involved in the protection against cardiorenal fibrosis seen in *TKO*, AngII-infused *TKO*, and AngII-infused *Vav1*$^{-/-}$ mice.

T_{REG} cells promote protection against hypertension-driven cardiorenal fibrosis. In view of the results presented above, we decided to investigate the possible implication of T_{REG} cells in the protection against hypertension-driven cardiorenal fibrosis shown by *Vav1*$^{-/-}$ mice. As a first step, we decided to analyze whether an artificial increase in the T_{REG}/T_H ratio in *WT* mice could reproduce the protection against cardiorenal fibrosis offered by the *Vav1* gene deficiency. To this end, we generated *in vitro* T_{REG} cells (referred to below as iT_{REG} cells) by culturing *WT* splenic CD4$^+$ CD25$^-$ lymphocytes in the presence of a differentiation cocktail and, upon purification by flow cytometry (Fig. 4A, second and third panels from left), injected them into *WT* recipient mice. We carried out two independent control experiments to make sure that this approach led to effective changes in the T_{REG}/T_H cell ratio in recipient mice. First, we confirmed by flow cytometry that we were actually injecting T_{REG} cells; ≈80% of the cells differentiated *in vitro* were positive for the T_{REG} cell-specific transcriptional factor Foxp3 (Fig. 4A, right). Second, by pilot experiments in which we injected iT_{REG} cells generated from C57BL/6 Ly5.1 mice (whose hematopoietic cells are CD45.1$^+$) into *WT* C57BL/10 mice (whose hematopoietic cells are CD45.2$^+$), we could estimate that the experimental protocol chosen does promote 3- and 2-fold increases in the total numbers of T_{REG} cells in recipient mice during the first six days and at late times postinjection, respectively (Fig. 4B, filled squares). These variations are derived directly from the iT_{REG} cells (CD45.1$^+$) that had been injected into mice (Fig. 4B, open squares). Moreover, we found that the injected iT_{REG} population maintains the CD4$^+$ CD25$^+$ status over an extended period, although it undergoes a 2-fold decrease at the latest time point analyzed (Fig. 4C, light blue squares). As a result, we calculated that the injected animals maintain high T_{REG}/non-T_{REG} CD4$^+$ cell ratios during most of the time course used in these studies (Fig. 4C, compare light blue and light red squares at each time point). When we repeated these injection experiments with standard CD57BL/10 iT_{REG} cells, we observed that the *WT* recipient mice exhibited no cardiorenal fibrosis (Fig. 4D and E) and a buffered hypertensive response (Fig. 4F) upon systemic administration of AngII. Based on the results obtained in the analyses of hematopoietic cells present in Vav family knockout mice (Table 1), we also decided to include as an additional readout in these studies the evolution of neutrophil numbers in the kidneys of iT_{REG}-injected mice. We observed a significantly lower percentage of neutrophils in the kidneys of these mice than in those of the controls (Fig. 4G and H), suggesting a possible direct link between the elevated T_{REG}/T_H ratios and the kidney neutropenia inferred earlier from the experiments with *TKO* mice (Table 1). Interestingly, the latter effect is also observed in mice that were not treated with AngII (Fig. 4I), possibly indicating hypertension-independent cross talk between T_{REG} cells and neutrophils in this

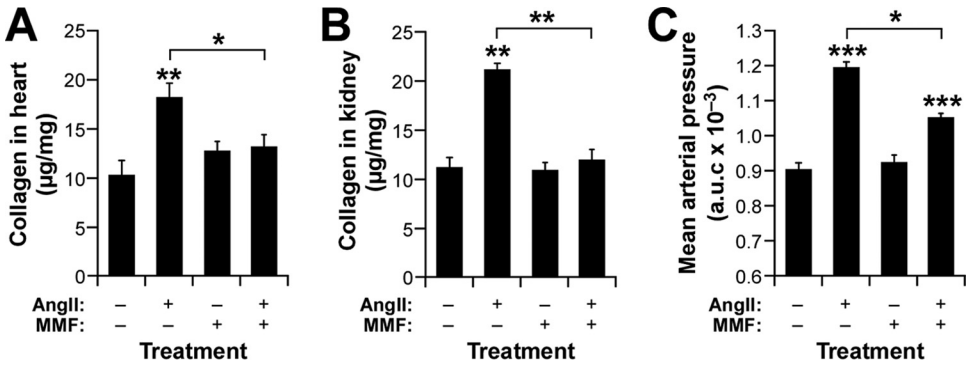

FIG 3 MMF protects immunodeficient mice against cardiorenal fibrosis. (A to C) Cardiorenal fibrosis levels (A and B) and area under the curve (AUC) for blood pressure (C) developed by *Foxn1*^{nu} mice after a 14-day treatment with the indicated agents. Asterisks indicate significant differences (*, $P \leq 0.05$; **, $P \leq 0.01$; ***, $P \leq 0.001$) from the control or between the indicated experimental groups ($n = 6$).

tissue. Using a similar experimental approach, we demonstrated that Vav1 expression is not important for the efficient generation (Fig. 4J) and functionality (Fig. 4K) of iT_{REG} cells in this experimental setting. Thus, it is unlikely that the phenotype observed in *Vav1*$^{-/-}$ mice could be caused directly by the presence of nonfunctional T_{REG} cells in the kidneys.

To further confirm the implication of T_{REG} cells in this process, we next assessed the effect of eliminating T_{REG} cells in *Vav1*$^{-/-}$ mice. According to our hypothesis, such a procedure would restore fibrosis in the kidneys of these animals and induce a concomitant increase in the number of intrarenal neutrophils. To achieve this end, we carried out an immunodepletion strategy consisting of injecting the animals under study with an antibody to the high-affinity interleukin 2 receptor (CD25). As shown in Fig. 5A, this procedure promotes efficient and long-term elimination of T_{REG} cells in mice. We observed that when infused with

TABLE 1 Percentages of hematopoietic subpopulations in mice of various genotypes

Tissue and cell type	% of total hematopoietic cells in mice of genotype[a]:			
	WT	*DKO*	*TKO*	*Vav1*$^{-/-}$
Kidney				
$CD11b^+$ $Gr1^+$ neutrophils	0.37 ± 0.07	**0.91 ± 0.17***	**0.1 ± 0.03*†**	**0.15 ± 0.01*†**
$CD4^+$ T cells	0.14 ± 0.02	0.13 ± 0.01	**0.02 ± 0.005*†**	**0.02 ± 0.000*†**
$CD4^+$ $Foxp3^+$ T_{REG} cells	0.06 ± 0.03	0.07 ± 0.02	0.02 ± 0.003	0.01 ± 0.002
$CD11b^+$ $F4/80^+$ macrophages	0.69 ± 0.16	0.73 ± 0.11	0.45 ± 0.07	ND
$CD11c^+$ dendritic cells	0.26 ± 0.04	0.26 ± 0.04	0.3 ± 0.03	ND
$CD11c^-$ dendritic cells	0.16 ± 0.04	0.17 ± 0.05	0.14 ± 0.03	ND
$CD8^+$ T cells	0.60 ± 0.06	0.68 ± 0.047	0.643 ± 0.031	ND
$B220^+$ B cells	18.80 ± 1.09	18.98 ± 1.75	18.467 ± 2.17	ND
Blood				
$CD11b^+$ $Gr1^+$ neutrophils	18.30 ± 2.6	**48.20 ± 2.60***	**46.3 ± 7*†**	12.1 ± 1.3
$CD4^+$ T cells	22.08 ± 2.11	29.24 ± 3.10	**7.43 ± 0.14*†**	**5.73 ± 0.21*†**
$CD4^+$ $Foxp3^+$ T_{REG} cells	1.22 ± 0.21	2.46 ± 0.36	1.63	1.35 ± 0.04
$CD8^+$ T cells	16.07 ± 0.91	7.67 ± 1.94	**4.03 ± 1.35*†**	**6.09 ± 0.72*†**
$B220^+$ B cells	29.25 ± 9.33	**12.24 ± 3.65***	**7.92 ± 2.01***	**7.34 ± 2.96***
Spleen				
$CD4^+$ T cells	10.07 ± 0.48	12.17 ± 1.67	**3.77 ± 0.44*†**	**4.35 ± 0.32*†**
$CD4^+$ $Foxp3^+$ T_{REG} cells	1.04 ± 0.065	0.95 ± 0.02	0.91 ± 0.02	1.11 ± 0.079
$CD8^+$ T cells	10.60 ± 0.69	8.52 ± 0.37	**3.43 ± 0.49*†**	**3.41 ± 0.17*†**
$B220^+$ B cells	70.25 ± 1.19	71.4 ± 1.9	**33.7 ± 2.84*†**	**26.2 ± 3.08*†**
Thymus				
$CD4^+$ $CD8^-$ T cells	9.71 ± 0.53	9.34 ± 0.64	**2.77 ± 0.25*†**	**5.21 ± 1.07*†**
$CD4^+$ $Foxp3^+$ T_{REG} cells	0.49 ± 0.04	0.39 ± 0.06	0.29 ± 0.06	0.6 ± 0.18
$CD4^-$ $CD8^+$ T cells	6.57 ± 2.03	2.93 ± 0.32	**1.8 ± 0.19*†**	**3.39 ± 0.68*†**
$CD4^+$ $CD8^+$ thymocytes	75.3 ± 1.96	80.5 ± 1	**40.23 ± 1.52*†**	**59.3 ± 5.57*†**
$CD4^-$ $CD8^-$ thymocytes	8.24 ± 0.86	7.24 ± 0.3	**55.17 ± 1.52*†**	**31.6 ± 5.16*†**

[a] The percentages of the indicated cells in the total population analyzed were determined by flow cytometry (see Materials and Methods). Results are means ± standard deviations for six mice per genotype. Values that are statistically significantly different from those for *WT* mice are shown in boldface. Asterisks and daggers indicate significant differences ($P \leq 0.05$) from results for *WT* and *DKO* mice, respectively. ND, not determined.

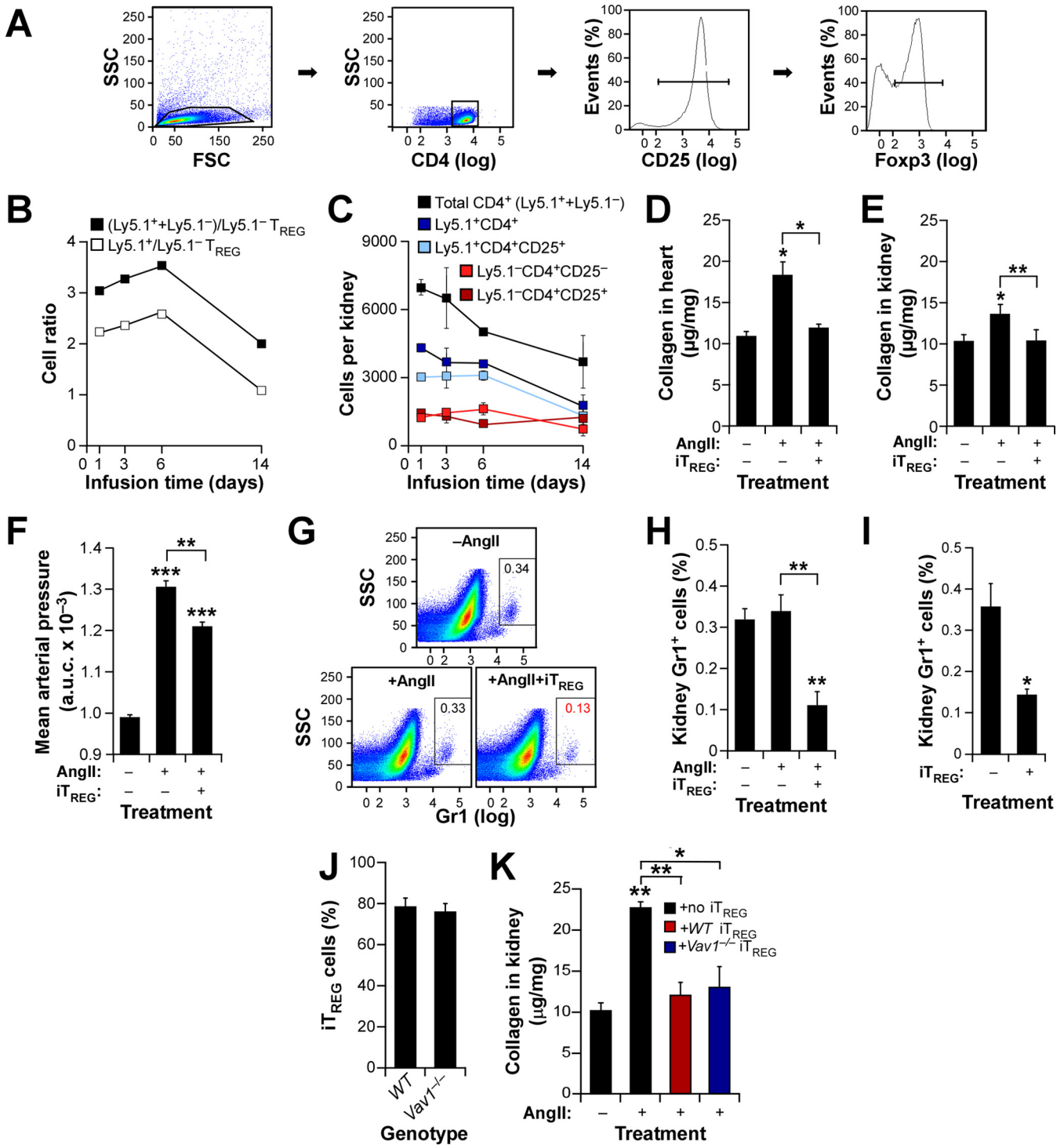

FIG 4 Increased T_{REG}/T_H cell ratios protect against AngII-triggered cardiorenal fibrosis. (A) Example of purified iT_{REG} cells used in these experiments. $CD4^+$ cells obtained from homogenized spleens and separated by flow cytometry (two left panels) were cultured with antibodies to CD3, CD28, interleukin 2, and transforming growth factor β_1. After 4 days, CD25 expression was checked by flow cytometry (third panel from left) and injected into mice. In some cases, aliquots of cells were checked for Foxp3 expression (right panel). (B) Ratios of the indicated cell populations in kidneys from animals injected with 2×10^5 $Ly5.1^+$ T_{REG} cells and infused 24 h later with AngII for the indicated periods. (C) Mean numbers of the indicated cell populations in kidneys from mice used in the experiment for which results are shown in panel B ($n = 4$). (D to F) Cardiorenal fibrosis levels (D and E) and AUC for mean arterial pressure (F) in *WT* mice maintained under the indicated conditions for 14 days. Asterisks indicate significant differences (*, $P \leq 0.05$; **, $P \leq 0.01$; ***, $P \leq 0.001$) from the control or between the indicated experimental groups ($n = 4$). (G and H) Representative example (G) and quantification (H) of neutrophils in kidneys from *WT* mice at the end of the experiments described in the legend to panel B. Asterisks indicate significant differences (**, $P \leq 0.01$) from the control or between the indicated experimental groups ($n = 4$). (I) Quantification of kidney-resident neutrophils in *WT* mice treated as indicated. *, $P \leq 0.05$ ($n = 4$). (J) Percentages of iT_{REG} cells generated from splenic *WT* and *Vav1*$^{-/-}$ $CD4^+$ $CD25^-$ T cells in cell culture ($n = 4$). (K) Extent of kidney fibrosis in AngII-infused *Foxn1*^{nu} mice injected with the indicated iT_{REG} cells. Asterisks indicate significant differences (*, $P \leq 0.05$; **, $P \leq 0.01$) from the control or between the indicated experimental groups ($n = 4$).

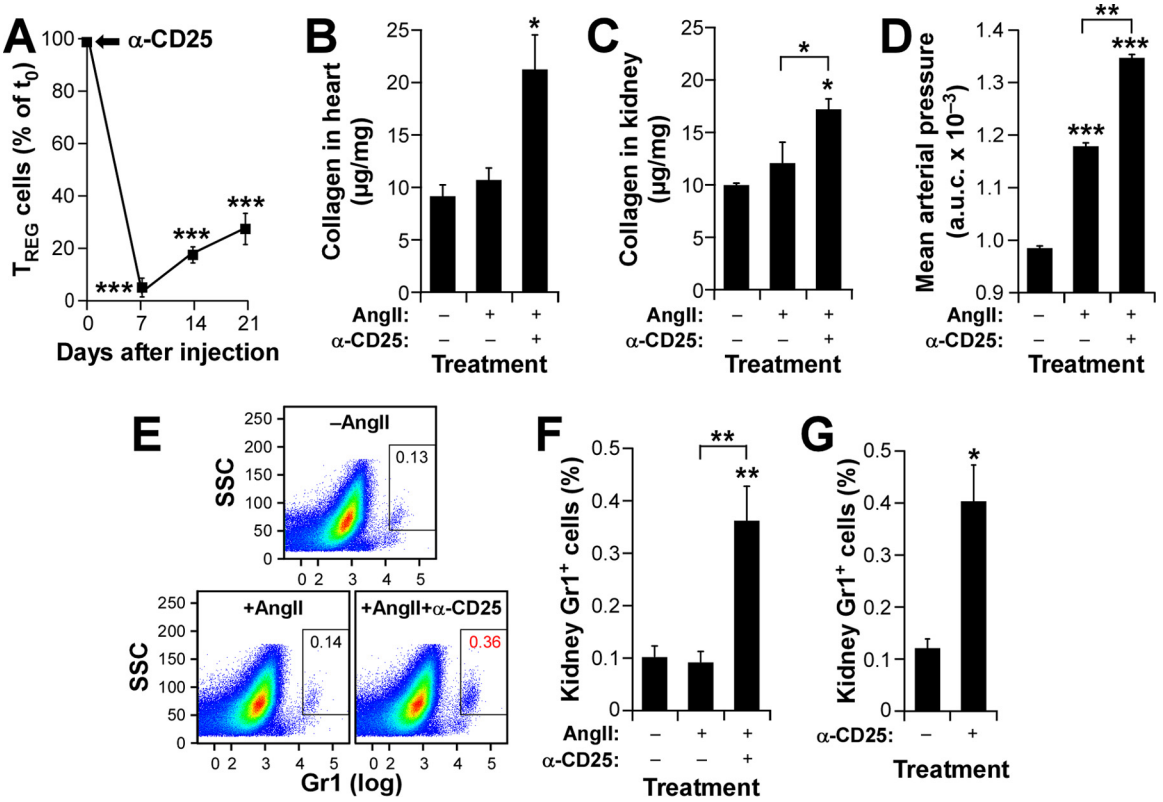

FIG 5 Immunodepletion of T_{REG} cells restores renal fibrosis in Vav1-deficient mice. (A) Evolution of the CD4$^+$ CD25$^+$ cell population in *Vav1*$^{-/-}$ mice upon immunodepletion with antibodies to CD25. The time of injection (t_0) is indicated by an arrow. ***, $P \leq 0.001$ ($n = 4$). (B to D) Cardiorenal fibrosis levels (B and C) and AUC for mean arterial pressure (D) in *Vav1*$^{-/-}$ mice treated as indicated. Asterisks indicate significant differences (*, $P \leq 0.05$; **, $P \leq 0.01$; ***, $P \leq 0.001$) from the control or between the indicated experimental groups ($n = 4$). (E and F) Representative example (E) and quantification (F) of neutrophils in kidneys from *Vav1*$^{-/-}$ mice used in the experiments for which results are shown in panels A to D. Asterisks indicate significant differences (**, $P \leq 0.01$) from the control or between the indicated experimental groups ($n = 4$). (G) Quantification of kidney-resident neutrophils in *Vav1*$^{-/-}$ mice under the indicated conditions. *, $P \leq 0.05$ ($n = 4$).

AngII, T_{REG} cell-immunodepleted *Vav1*$^{-/-}$ mice behave like *WT* mice in terms of cardiorenal fibrosis development (Fig. 5B and C) and blood pressure elevation (Fig. 5D). Importantly, we found that these mice also recover WT-like percentages of kidney-resident neutrophils under both AngII administration (Fig. 5E and F) and basal (Fig. 5G) conditions. In addition to further confirming the negative cross talk between T_{REG} cells and neutrophils, these results suggest that the intrarenal neutropenia detected earlier in both AngII-treated and untreated *Vav1*$^{-/-}$ mice (Table 1 and Fig. 4) cannot be caused by intrinsic signaling dysfunctions of *Vav1*$^{-/-}$ neutrophils. Collectively, these findings support the idea of a direct functional link between T_{REG}/T_H ratios and neutrophil numbers that eventually modulates AngII-driven tissue fibrosis in hypertensive mice.

Neutrophils contribute to hypertension-driven cardiorenal fibrosis. Given the direct correlation between effective fibrosis development and neutrophil numbers observed in the experiments described above, we next decided to address the direct contribution of these myeloid cells to this process. To this end, we immunodepleted them in *WT* mice by injections with an antibody (1A8) to the Ly6G subunit of the Gr1 antigen. The efficient depletion of these cells was confirmed by detecting the percentages of Gr1$^+$ cells in the blood of injected animals by using flow cytometry analyses (Fig. 6A). Using this approach, we observed that neutrophil-depleted *WT* mice phenocopy the *Vav1* gene deficiency in terms of protection against cardiorenal fibrosis (Fig. 6B and C) and the development of mild hypertensive responses (Fig. 6D) upon systemic infusion with AngII. This effect is neutrophil dependent, as evidenced by the fact that the kidneys of mice pretreated with antibody 1A8 exhibit percentages of macrophages (Fig. 6E) and CD4$^+$ T cells (Fig. 6F) similar to those found in control mice. However, under the same conditions, they show the expected lack of neutrophils in this organ (Fig. 6G and H). These results indicate that neutrophils are critical for the induction of all AngII-triggered pathophysiological responses, even in fully immunocompetent mice.

T_{REG} cells protect immunodeficient mice against hypertension-driven fibrosis. To further rule out the possibility that the antifibrotic effect of iT_{REG} cells was independent of their roles in general T cell immunosuppression, we decided to repeat some of the experiments described above with AngII-infused SCID/beige (C.B-17/lcrHsd-*Prkdc*^{scid}*Lyst*$^{bg\text{-}J}$) and *Foxn1*^{nu} mice. SCID/beige mice are totally devoid of T and B lymphocytes due to a SCID mutation that impairs the V(D)J recombination of antigen receptor genes in these two cell lineages. They also have diminished natural killer cell and macrophage activity owing to the presence of the beige mutation. As controls for these animals, we used immunocompetent mice of the same genetic background (BALB/c).

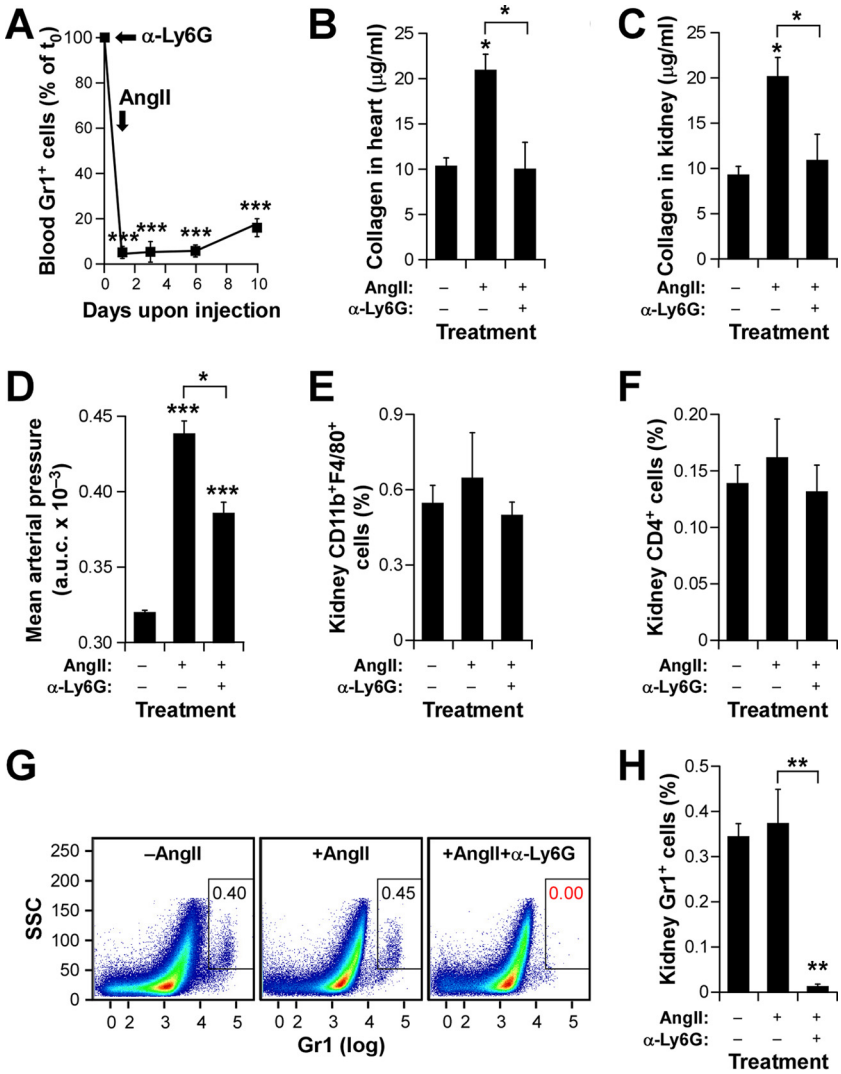

FIG 6 Neutrophils are involved in AngII-driven cardiorenal fibrosis. (A) Impact of the immunodepletion step on the numbers of neutrophils in *WT* mice. ***, $P \leq 0.001$ ($n = 4$). The time points of antibody injection (α-Ly6G) and implantation of osmotic pumps (AngII) are indicated by arrows. (B and C) Extent of cardiorenal fibrosis obtained in *WT* animals injected with either a control antibody or an anti-Ly6G antibody and subsequently infused with AngII as indicated. Asterisks indicate significant differences (*, $P \leq 0.05$) from the control or between the indicated experimental groups ($n = 4$). (D) AUC for the mean arterial pressure increase obtained in the experiment for which results are shown in panels A to C. Asterisks indicate significant differences (*, $P \leq 0.05$; ***, $P \leq 0.001$) from the control or between the indicated experimental groups ($n = 4$). (E and F) Quantification of kidney-resident macrophages (E) and $CD4^+$ T cells (F) at the end of these experiments. (G and H) Representative dot plots (G) and quantification (H) of neutrophils present in kidneys at the end of these experiments. Asterisks indicate significant differences (**, $P \leq 0.01$) from the control or between the indicated experimental groups ($n = 4$).

In agreement with our results with *WT* C57BL/10 animals (Fig. 4), we observed that injection of iT_{REG} cells promotes protection against AngII-induced renal fibrosis in SCID/beige (Fig. 7A to C), BALB/c (Fig. 7A to C), and *Foxn1*^{nu} (Fig. 7D and E, red bars) mice. These effects are associated with parallel reductions in the normal percentages of neutrophils present in the kidneys of those animals (Fig. 7F to H). As a negative control, we did not observe any significant protection upon injection of equal numbers of $CD4^+$ $CD25^-$ lymphocytes into *Foxn1*^{nu} mice (Fig. 7D, E, and H, blue bars). Conversely, similar protection is obtained upon the immunodepletion of neutrophils (Fig. 7F and G) in SCID/beige and BALB/c mice (Fig. 7A to C).

Taking the results presented above into account, we decided to investigate whether the antifibrotic effects observed with the immunosuppressant MMF in the T cell-immunodeficient *Foxn1*^{nu} strain (Fig. 3) could also involve alterations in either the number or the functionality of neutrophils. We observed that treatment with this drug does not induce any significant effect on the neutrophils of *Foxn1*^{nu} mice under normal conditions. However, MMF does promote a severe and systemic neutropenic effect when combined with AngII administration (Fig. 7I). Taken together, these findings indicate that the protective effects against tissue fibrosis observed with the *Vav1* deficiency, iT_{REG} cells, and MMF can probably all be integrated in a common mechanistic framework whose endpoint is the control of the numbers of either tissue-resident (in the case of *Vav1*-deficient and iT_{REG}-injected *WT* mice) or systemic (in the case of MMF treat-

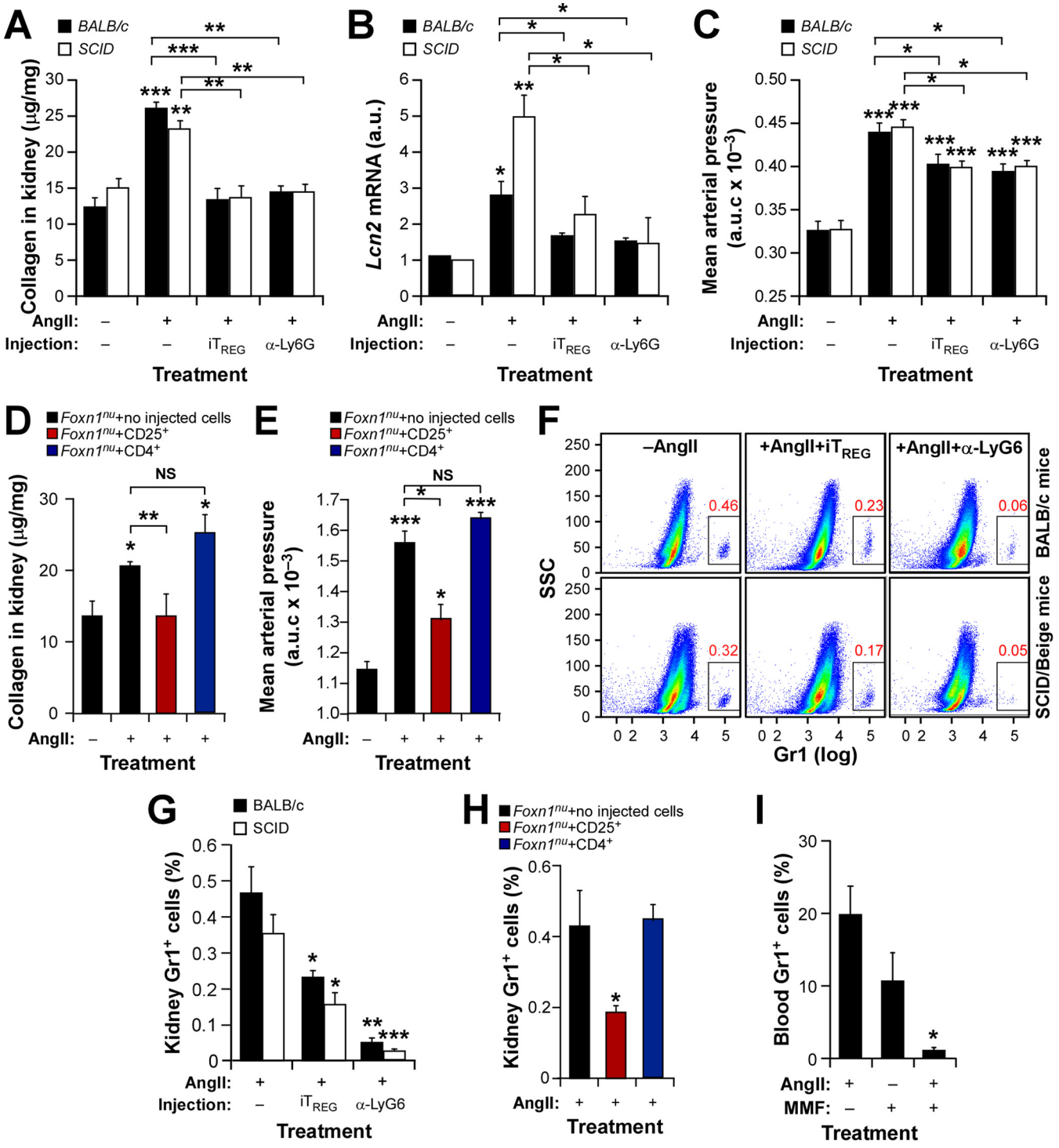

FIG 7 T_{REG} cells protect against hypertension-driven fibrosis in an immunosuppression-independent manner. (A to E) Renal fibrosis (A and D), abundance of *Lcn2* transcripts in kidneys (B), and AUC for mean arterial pressure levels (C and E) in the indicated mouse strains under the indicated treatment conditions. Asterisks indicate significant differences (*, $P \leq 0.05$; **, $P \leq 0.01$; ***, $P \leq 0.001$) from the control or between the indicated experimental groups ($n = 4$). (F and G) Representative dot plots (F) and quantification (G) of kidney-resident neutrophils in the indicated mouse strains under the indicated treatment conditions. Asterisks indicate significant differences (*, $P \leq 0.05$; **, $P \leq 0.01$; ***, $P \leq 0.001$) from the control or between the indicated experimental groups ($n = 4$). (H and I) Percentages of kidney-resident and circulating neutrophils in *Foxn1*^{nu} mice under the indicated experimental conditions. Asterisks indicate significant differences (*, $P \leq 0.05$) from the control ($n = 4$).

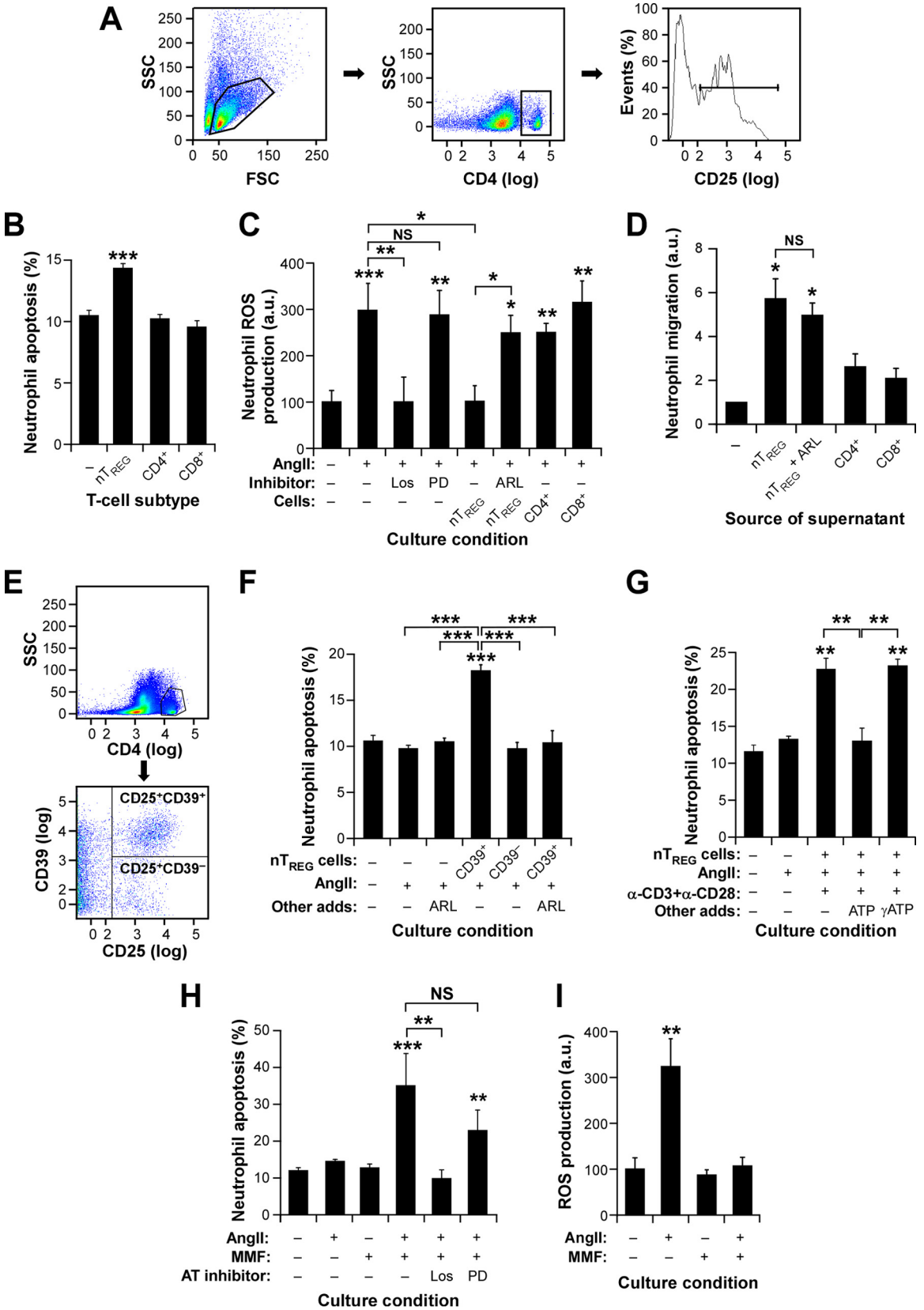

FIG 8 T_{REG} cells induce CD39-dependent neutrophil apoptosis. (A) Example of the flow cytometry purification step for obtaining the splenic $CD4^+$ $CD25^+$ nT_{REG} cells used in the experiments for which results are shown in panels B to D. (B and C) Apoptotic response (B) and ROS production (C) of neutrophils under the indicated *in vitro* conditions. ARL, ARL 67156; $CD4^+$, $CD4^+$ $CD25^-$ T cells; $CD8^+$, $CD8^+$ T cells; Los, losartan; PD, PD123319. Asterisks indicate significant

ment) neutrophils. Furthermore, they indicate that this T_{REG}/neutrophil axis confers cardiorenal protection using immunosuppression-independent mechanisms.

T_{REG} cells promote direct apoptosis of neutrophils in a CD39-dependent manner. Although our results with both *Foxn1^{nu}* and SCID/beige mice excluded the participation of conventional T cells in this response, they could not formally rule out the possibility that other T_{REG} cell partners, such as macrophages or dendritic cells, could indirectly mediate the negative effects of T_{REG} cells on neutrophil numbers. Such an idea is, in fact, consistent with previous findings indicating that T_{REG} cells can mediate both acute lung injury-induced fibrosis and some pathogen-triggered inflammatory responses by influencing the activity of non-T-cell hematopoietic lineages (40, 41). To tackle this issue, we decided to investigate the effects of T_{REG} cells, AngII, and MMF on both the viability and the function of neutrophils by using cell culture experiments. To this end, we first analyzed the effect of coculturing primary bone marrow neutrophils with splenic $CD4^+$ $CD25^+$ T cells that were directly obtained from mice using flow cytometry purification procedures. The latter cells are referred to as natural T_{REG} (nT_{REG}) cells in order to distinguish them from the *in vitro*-differentiated iT_{REG} cells used in earlier experiments. An example of the purification of these cells can be found in Fig. 8A. These experiments revealed that neutrophils exhibit increased apoptotic rates when cultured in the presence of nT_{REG} cells (Fig. 8B), an effect that was independent of the presence of AngII in the culture medium (Fabbiano, unpublished). Probably as a result of this apoptotic effect, we also found that the presence of nT_{REG} cells leads to the elimination of the production of reactive oxygen species (ROS), which is stimulated by AngII in neutrophils (Fig. 8C). ROS production is mediated by the AngII AT_1 receptor in neutrophils, as evidenced by the fact that this response can be blocked by an AT_1 receptor antagonist (losartan) but not by an AT_2 receptor antagonist (PD123319) (Fig. 8C). Additional experiments indicated that nT_{REG} cells are not involved exclusively in the negative regulation of neutrophils. For example, we observed that supernatants from nT_{REG} cultures can promote the chemotaxis of primary neutrophils (Fig. 8D). All these actions seem to be nT_{REG} specific, because no significant effects were observed when T_H ($CD4^+$) and cytotoxic ($CD8^+$) T lymphocytes (Fig. 8B to D) were used in these experiments. Thus, in agreement with the observations made *in vivo*, the present results indicate that T_{REG} cells control the viability of primary neutrophils in an AngII-independent manner.

T_{REG} cells can inhibit other cell types using a number of signaling mechanisms, including cytotoxic-T-lymphocyte-associated antigen 4 (CTLA4)-mediated immunosuppression, granzyme- and perforin-dependent cytotoxicity, cytokine-based paracrine signaling, and the degradation of extracellular ATP using the ecto-ATP diphosphohydrolase activity of plasma membrane-localized CD39 molecules (1, 2). We ruled out the three former mechanisms, because our results indicated that the T_{REG}-neutrophil interconnection was probably associated with an immunosuppression-independent proapoptotic mechanism (Fig. 7 and 8B). We also excluded a paracrine-dependent proapoptotic effect, given our observations indicating that the supernatants obtained from nT_{REG} cell cultures promote the chemotaxis rather than the apoptosis of neutrophils (Fig. 8D). These observations led us to consider the possible implication of CD39, a surface molecule expressed by 50% ± 7% and 58% ± 6% of the iT_{REG} and splenic nT_{REG} cells used in this work, respectively (in 4 independent experiments). This percentage is further expanded to 71.7% ± 4.1% of the whole iT_{REG} population when AngII is added to the *in vitro* T_{REG} differentiation cocktail (in 4 independent experiments) ($P \leq 0.05$). To test this idea, we purified and separated splenic $CD39^+$ and $CD39^-$ nT_{REG} cells by flow cytometry (Fig. 8E) and subsequently cultured them with primary bone marrow neutrophils. Using this approach, we observed that the $CD39^+$ nT_{REG} cell population, but not the $CD39^-$ nT_{REG} cell population, prompts the apoptosis of neutrophils (Fig. 8F). This proapoptotic effect is eliminated when the ATPase activity of this ectoenzyme is blocked in those cultures with either a CD39 drug inhibitor (ARL 67156) (Fig. 8F) or an excess of its normal catalytic substrate (ATP) (Fig. 8G). As control, no rescue is observed when the T_{REG}-neutrophil cultures are supplemented with a nonhydrolyzable form of ATP (adenosine 5′-[γ-thio]triphosphate) (Fig. 8G). In agreement with these results, we found that ARL 67156 eliminates the negative effect of nT_{REG} cells on ROS production by AngII-stimulated neutrophils (Fig. 8C). In contrast, ARL 67156 does not block other T_{REG} cell activities, such as neutrophil chemotaxis (Fig. 8D). ARL 57156 (Fig. 8F) and ATP (Fig. 8G) cannot prevent the basal apoptotic rates typically exhibited by neutrophils in cell culture, either, further confirming that their effects are CD39 dependent.

We next investigated whether the neutropenic effect found in MMF-treated mice could result from some direct action of the drug on primary neutrophils. As shown in Fig. 8H, MMF has no effect on the viability of these cells under normal culture conditions. However, MMF promotes enhanced apoptotic rates when used in AngII-stimulated neutrophil cultures (Fig. 8H). This goes in parallel with the elimination of ROS production by the stimulated neutrophils (Fig. 8I). In agreement with the stimulation-dependent effect of MMF, its proapoptotic effect is lost when the stimulated neutrophils are pretreated with losartan but not PD123319 (Fig. 8H). Taken together, these results indicate that the neutropenia observed in *TKO* mice, *Vav1$^{-/-}$* mice, and nude mice treated with AngII plus MMF is probably due to a direct proapoptotic cell-autonomous effect of both $CD39^+$ T_{REG} cells and MMF on neutrophils.

$CD39^+$ T_{REG} cells protect against AngII-driven hypertension and its comorbidities. To corroborate the physiological relevance of the *in vitro* culture experiments described in the preceding section, we investigated the actual contribution of $CD39^+$ T_{REG} cells to the cardiovascular and renal parameters under study in this work. To this end, we first decided to analyze the effect of injecting

differences (*, $P \leq 0.05$; **, $P \leq 0.01$; ***, $P \leq 0.001$) from the control or between the indicated experimental groups ($n = 4$). (D) Effect of T_{REG} cell-derived culture supernatants on neutrophil chemotaxis (values obtained with medium alone were given an arbitrary value of 1). Asterisks indicate significant differences (*, $P \leq 0.05$) from the control; NS, no significant difference ($n = 4$). (E) Example of the purification step used to obtain the splenic $CD39^+$ and $CD39^-$ nT_{REG} cells used in the experiment for which results are shown in panel F. (F to H) Apoptotic responses of neutrophils under the indicated culture conditions. $CD39^+$, $CD4^+$ $CD25^+$ $CD39^+$ nT_{REG} cells; $CD39^-$, $CD4^+$ $CD25^+$ $CD39^-$ nT_{REG} cells; α-CD3 and α-CD28, antibodies to mouse CD3 and CD28, respectively. Asterisks indicate significant differences (**, $P \leq 0.01$; ***, $P \leq 0.001$) from the control or between the indicated experimental groups ($n = 4$). (I) AngII-stimulated ROS production by neutrophils under the indicated culture conditions. Asterisks indicate significant differences (**, $P \leq 0.01$) from the control ($n = 4$).

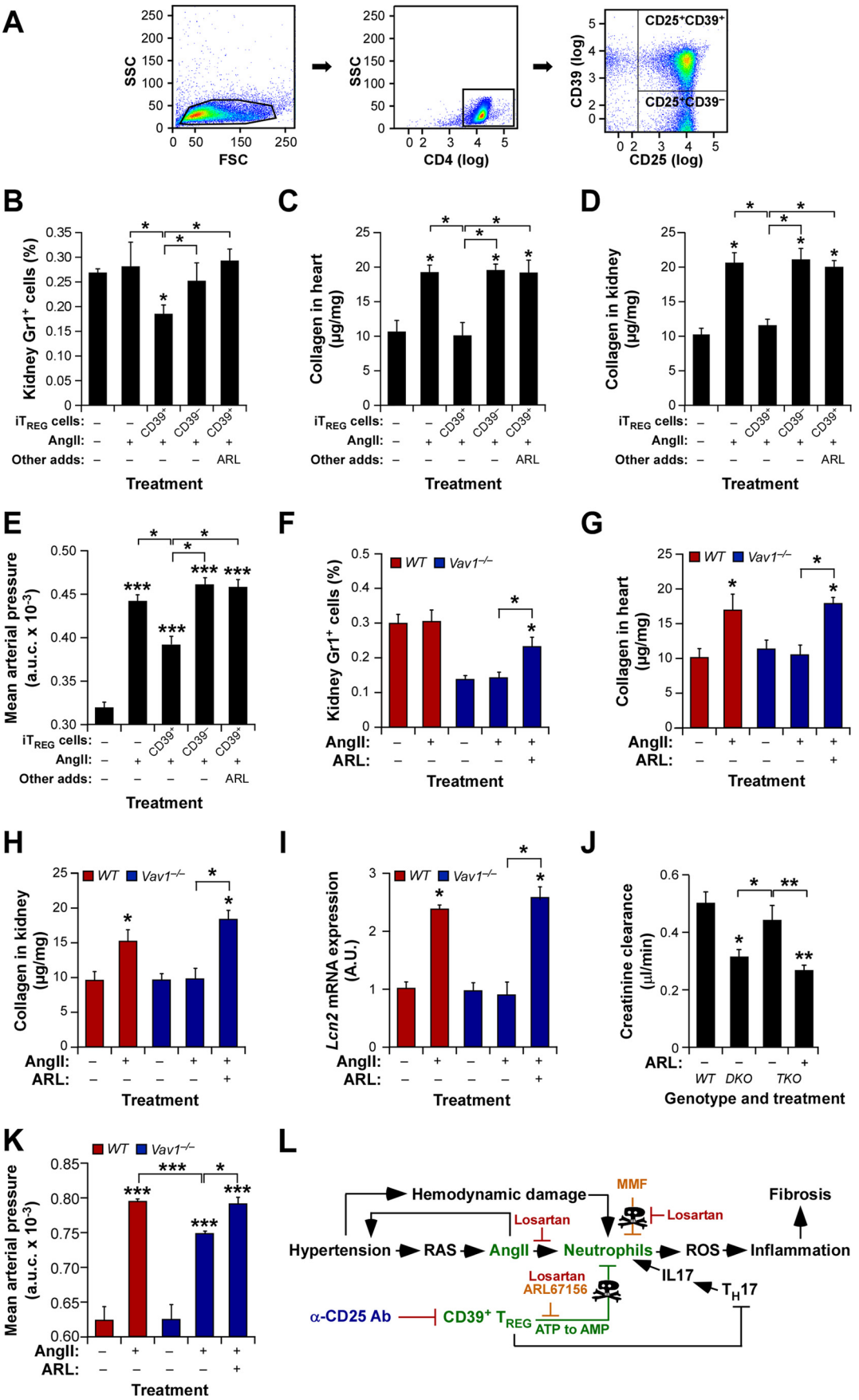

flow cytometry-purified $CD39^+$ and $CD39^-$ iT_{REG} cells (Fig. 9A) on the AngII-mediated fibrosis of *WT* mice. We observed that the $CD39^+$ iT_{REG} subset does promote kidney neutropenia (Fig. 9B), protection against cardiorenal fibrosis (Fig. 9C and D), and the expected buffering effect on arterial blood pressure elevation (Fig. 9E) in recipient mice. However, such activity was not observed when $CD39^-$ iT_{REG} cells were injected into *WT* mice (Fig. 9B to E). Further underscoring the role of the CD39 ectoenzyme in this process, we found that the effect induced by the injected $CD39^+$ iT_{REG} cells is abolished when the recipient mice are treated with ARL 57156 (Fig. 9B to E). Confirming the implication of these cells in the phenotype shown by knockout mice, we found that the administration of this CD39 inhibitor to AngII-treated *Vav1*$^{-/-}$ mice mimicked the effects of the T_{REG} immunodepletion already seen in those mice, including the restoration of increased numbers of kidney-resident neutrophils (Fig. 9F), the development of fibrosis in both the heart (Fig. 9G) and the kidneys (Fig. 9H), elevated levels of *Lcn2* mRNA expression in the kidneys (Fig. 9I), reductions in creatinine clearance by the kidneys (Fig. 9J), and the restoration of a full hypertensive response (Fig. 9K). Collectively, these results indicate that T_{REG} cells are involved in protection against hypertension-driven cardiorenal fibrosis using a nonconventional, CD39- and neutrophil-dependent mechanism (Fig. 9L).

DISCUSSION

Our results have unveiled a hitherto unknown $CD39^+$ T_{REG} cell/neutrophil-based mechanism that probably represents a first trench of protection against AngII-elicited heart remodeling and cardiorenal fibrosis (Fig. 9L). This mechanism has been found to be operative under both normotensive and hypertensive conditions, suggesting that it may be involved in the homeostatic control of neutrophil numbers in some specific tissues. The utilization of a $CD39^+$ T_{REG} cell/neutrophil axis seems *prima facie* a good functional strategy for the control of these pathophysiological processes, because evidence from other fibrosis-associated kidney dysfunctions indicates that neutrophils act as critical "decision-shapers" during the inflammation-based priming phase of the fibrotic process (8). Furthermore, they are highly dependent on the availability of both extracellular ATP and ADP for a large variety of functions, including survival, chemotaxis, and other inflammation-connected functions (42). Interestingly, this antifibrotic mechanism seems to be quite specific, since it does not confer protection under L-NAME-triggered hypertension conditions. Since *Vav1*$^{-/-}$ mice show increased T_{REG}/T_H cell ratios and neutropenia prior to the hypertension step, it is likely that this differential response is due to the engagement of different proinflammatory or profibrotic routes upon systemic administration of AngII and L-NAME. Likewise, we have observed that this antifibrotic mechanism does not prevent the arterial remodeling that typically develops under AngII-driven hypertension conditions. This is consistent with previous results indicating that this response may involve either macrophages or a nonconventional $CD3^+$ $CD4^-$ $CD8^-$ T cell subpopulation (15, 20).

It is worth noting that this new regulatory layer involved in fibrotic responses does not exclude the participation of T_H cells and other myeloid cells further downstream in the fibrotic pathophysiological cascade. On the contrary, our observations suggest that this first T_{REG}-dependent barrier of defense against AngII-driven tissue fibrosis is probably overcome under chronic hypertension conditions by the subsequent recruitment and/or activation of either T_H cell subtypes or downstream proinflammatory responses providing that normal T_{REG}/T_H ratios are preserved in mice (Fig. 9L). In any case, the protection shown by T_{REG} cell-transplanted *WT* mice suggests that therapies based on either alterations of T_{REG}/T_H cell ratios (i.e., via either allogeneic T_{REG} cell transfer or *in vivo* expansion of T_{REG} cells) or ATP/ADP depletion-dependent reduction of neutrophil numbers (i.e., using recombinant CD39 delivery techniques) could be valuable, either alone or in combination with AngII route inhibitors, for preventing cardiorenal fibrosis and the ensuing end-organ disease in patients with AngII-dependent hypertension.

Our results also suggest that previous findings regarding the positive effects of MMF and other immunosuppressants in hypertension-driven fibrosis (12, 13, 21) can be explained by the enhancement of this T_{REG}-dependent mechanism. In agreement with this, it has been shown that some of those immunosuppressants promote the peripheral expansion of T_{REG} cells (43, 44). The mechanism reported here could also be involved in both the fibrotic and the hypertensive effects induced by the transplantation and depletion of both conventional T and T_{REG} cells due to the changes in T_{REG}/T_H ratios intrinsically associated with these treatments (9, 10, 15–17). Interestingly, it has been reported that MMF treatment promotes neutropenia in some tissue-transplanted patients (45–47). Based on the present results, it would be interesting to determine whether this collateral effect could be caused by a similar mechanism to the one described here. It would be also worthwhile to pursue a better understanding of the proapoptotic effect of MMF on neutrophils. Given that this effect is observed only in an AngII- and AT_1 receptor-dependent manner, we surmise that MMF must create some metabolic imbalance in stimulated neutrophils. Whether this is done via in-target (inhibition of IMP dehydrogenase) or off-target effects of the drug remains to be determined. The effects of MMF in nonlymphoid cells have been described previously (39).

Interestingly, we have observed that the lack of tissue fibrosis in *TKO* and *Vav1*$^{-/-}$ mice is always associated with the development of milder hypertensive states under AngII-driven hypertension conditions (Fig. 9L). Our interpretation is that the latter effect is a downstream consequence of the lack of fibrosis and the subsequent preservation of normal renal functions in these mice. How-

FIG 9 $CD39^+$ T_{REG} cells are involved in the protection against AngII-driven cardiorenal dysfunctions. (A) Example of the flow cytometry-mediated purification of $CD39^+$ and $CD39^-$ iT_{REG} cells used in the experiments for which results are shown in panels B to E. (B to E) Percentages of kidney-infiltrating neutrophils (B), extent of cardiorenal fibrosis (C and D), and blood pressure levels (E) in *WT* mice under the indicated experimental conditions. Asterisks indicate significant differences (*, $P \leq 0.05$; **, $P \leq 0.01$; ***, $P \leq 0.001$) from the control or between the indicated experimental groups ($n = 4$). (F to K) Percentages of kidney-infiltrating neutrophils ($n = 4$) (F), cardiorenal fibrosis levels ($n = 4$) (G and H), abundance of *Lnc2* transcripts in kidneys ($n = 4$) (I), creatinine clearance rates ($n = 6$) (J), and overall blood pressure levels ($n = 4$) (K) in mice of the indicated genotypes under the indicated experimental conditions. Asterisks indicate significant differences (*, $P \leq 0.05$; **, $P \leq 0.05$; ***, $P \leq 0.001$) from the control or between the indicated experimental groups. (L) The new mechanism (green) described in this work. Inhibitors tested exclusively *in vitro* or *in vivo* are shown in red or blue letters, respectively. Those used under both conditions are shown in light brown letters. The T_{REG}-T_H-neutrophil connection is proposed on the basis of previously published data (1, 2, 7, 8, 22). RAS, renin-angiotensin system.

ever, given the highly intertwined connections between these two pathophysiological programs, it could also be argued that the mild hypertensive conditions are in fact responsible for the antifibrotic protection exhibited by these two mouse strains. Although it is difficult to formally exclude this possibility at the experimental level, we do not believe this alternative scenario is possible for three reasons. (i) We have observed that the arterial blood pressures of AngII-infused *WT* and *Vav1*$^{-/-}$ mice are rather similar during the early phases of the AngII infusion (0 to 6 weeks) and become statistically different only upon long-term exposure of animals to this vasopressor (10 to 15 weeks). Thus, from a kinetic point of view, it does not seem that the differential hypertension values could be the original cause of the lack of fibrosis in Vav1-deficient mice. (ii) We have found that the overall blood pressure levels of AngII-infused *Vav1*$^{-/-}$ and *TKO* mice are similar to those present in animals that do develop a full fibrotic response (i.e., untreated *DKO* mice). In agreement with this, we also have found that *TKO* (both untreated and AngII-treated) and *Vav1*$^{-/-}$ (AngII-treated) mice do develop other hypertension-associated dysfunctions, such as, for example, the thickening of the arterial media wall. (iii) We have seen that the time of divergence of blood pressure values between AngII-infused *WT* and *Vav1*$^{-/-}$ mice matches the time when the controls have already developed cardiorenal fibrosis (Fig. 2H), suggesting that the milder hypertension shown by untreated *TKO*, AngII-treated *TKO*, and AngII-infused *Vav1*$^{-/-}$ mice could be an effect of the lack of fibrosis development in these animals. This could originate either from a direct pressor effect of the lack of fibrosis or from the collateral engagement of other hypertension-linked processes that contribute to the pressure-natriuresis mechanism involved in long-term pressure control (i.e., production of aldosterone and vasopressin) (48). Regardless of the initial cause of the event, it is clear that the renal dysfunctions and the hypertensive state will eventually collaborate in a mutually reinforcing loop to ultimately determine the final arterial pressure and fibrosis state found in each of the control and test strains analyzed in the present study.

Outside the cardiovascular field, this work has also provided information about the role of Vav proteins in lymphocyte subpopulations and neutrophils. Thus, we have observed that Vav proteins seem to be dispensable for both T_{REG} cell development and effector functions, at least in the pathophysiological context studied in this work. This is in sharp contrast to the critical roles played by these proteins during the stepwise development, selection, and final effector stages of conventional $CD4^+$ and $CD8^+$ T cells (27, 28). Given that T_{REG} cells require low T cell receptor signals to undergo effective positive selection (49), this result suggests that Vav proteins probably contribute to establishing optimal thresholds of T cell receptor signaling during the intrathymic selection process rather being involved in yes/no digital decisions. The increased T_{REG}/T_H cell ratios present in Vav1-deficient mice may also explain the lack of autoimmunity present in Vav family-deficient mice despite their defects in negative selection (50). Such a property is specific for Vav proteins, because the elimination of other proximal T cell receptor signaling elements, such as Zap70 and Lat, does block T_{REG} cell development in the thymus (51, 52). We have also seen that a lack of Vav1 does not seem to significantly affect the overall functionality of neutrophils. In agreement with this, we have observed that the renal neutropenia found in these mice can be restored upon the immunodepletion of iT_{REG} cells. Conversely, a similar neutropenic effect can be induced when *WT* mice are injected with iT_{REG} cells. Additional experiments have also revealed that the AngII-mediated stimulation of neutrophil migration and ROS production is Vav1 independent (Fabbiano, unpublished). These data are in agreement with previous results from the lab of H. Welch indicating no major defects in the *in vivo* biological properties of *Vav1*$^{-/-}$ neutrophils (53, 54). It would be important, in any case, to continue the analyses of *Vav1*$^{-/-}$ T_{REG} cells and neutrophils in order to assess whether this protein plays some catalysis-dependent or independent roles in any of these cell types.

Taken together, these results provide a new biological perspective from which to understand the early steps involved in the ontogeny of cardiorenal fibrosis, one of the most fatal comorbidities associated with essential hypertension (5, 6). Given that other fibrosis- or T_{REG} cell-dependent diseases in the liver, lung, and muscle are influenced by AngII (8, 37), it would be interesting to investigate whether the T_{REG} cell/neutrophil axis reported here could also play protective roles against those conditions.

ACKNOWLEDGMENTS

We thank A. Abad, M. Blázquez, and the personnel of the CIC Microscopy, Pathology, and Cytometry units for technical assistance, M. Dosil for comments on the manuscript, and V. Tybulewicz and M. Turner for making available to us the initial stocks of *Vav1* and *Vav2* knockout mice, respectively.

This work has been supported by grants from the Castilla-León Autonomous Government (CSI101U13), the Spanish Ministry of Economy and Competitiveness (SAF2012-31371, RD12/0036/0002), Worldwide Cancer Research, the Solórzano Foundation, and the Ramón Areces Foundation to X.R.B. P.M. is funded by the Spanish Ministry of Economy and Competitiveness (SAF2011-27330). S.F., M.M.-M., J.R.-V., and A.M.-M. were supported by the Spanish Ministry of Economy and Competitiveness through BES-2010-031386, CSIC JAE-Doc, Juan de la Cierva, and BES-2009-016103 contracts, respectively. Spanish government-sponsored funding to X.R.B. is partially supported by the European Regional Development Fund.

We declare no competing interests.

S.F. participated in all the experimental work, analyzed data, and contributed to the artwork design and manuscript writing. M.M.-M. performed animal-based work, designed experiments, and analyzed data. J.R.-V. analyzed flow cytometry data and carried out histochemical analyses. M.P. and J.M.L.-N. performed experiments related to *in vivo* renal functions. M.A.S. and M.J.M. collaborated in blood pressure determination experiments. A.M.-M. and P.M. carried out work related to the characterization of kidney-resident hematopoietic cells. C.G.-M. performed and analyzed immunohistochemical experiments on tissue sections. B.A. helped in cell transplantation experiments with Ly5 mice. X.R.B. designed the work, analyzed data, wrote the manuscript, and carried out the final editing of figures.

REFERENCES

1. **Josefowicz SZ, Lu LF, Rudensky AY.** 2012. Regulatory T cells: mechanisms of differentiation and function. Annu Rev Immunol **30:**531–564. http://dx.doi.org/10.1146/annurev.immunol.25.022106.141623.
2. **Shevach EM.** 2009. Mechanisms of Foxp3$^+$ T regulatory cell-mediated suppression. Immunity **30:**636–645. http://dx.doi.org/10.1016/j.immuni.2009.04.010.
3. **Burzyn D, Benoist C, Mathis D.** 2013. Regulatory T cells in nonlymphoid tissues. Nat Immunol **14:**1007–1013. http://dx.doi.org/10.1038/ni.2683.
4. **Burzyn D, Kuswanto W, Kolodin D, Shadrach JL, Cerletti M, Jang Y, Sefik E, Tan TG, Wagers AJ, Benoist C, Mathis D.** 2013. A special population of regulatory T cells potentiates muscle repair. Cell **155:**1282–1295. http://dx.doi.org/10.1016/j.cell.2013.10.054.
5. **Kearney PM, Whelton M, Reynolds K, Muntner P, Whelton PK, He J.**

2005. Global burden of hypertension: analysis of worldwide data. Lancet **365:**217–223. http://dx.doi.org/10.1016/S0140-6736(05)70151-3.

6. **Lopez AD, Mathers CD, Ezzati M, Jamison DT, Murray CJ.** 2006. Global and regional burden of disease and risk factors, 2001: systematic analysis of population health data. Lancet **367:**1747–1757. http://dx.doi.org/10.1016/S0140-6736(06)68770-9.
7. **Liu Y.** 2011. Cellular and molecular mechanisms of renal fibrosis. Nat Rev Nephrol **7:**684–696. http://dx.doi.org/10.1038/nrneph.2011.149.
8. **Wynn TA, Ramalingam TR.** 2012. Mechanisms of fibrosis: therapeutic translation for fibrotic disease. Nat Med **18:**1028–1040. http://dx.doi.org/10.1038/nm.2807.
9. **Kvakan H, Kleinewietfeld M, Qadri F, Park JK, Fischer R, Schwarz I, Rahn HP, Plehm R, Wellner M, Elitok S, Gratze P, Dechend R, Luft FC, Muller DN.** 2009. Regulatory T cells ameliorate angiotensin II-induced cardiac damage. Circulation **119:**2904–2912. http://dx.doi.org/10.1161/CIRCULATIONAHA.108.832782.
10. **Barhoumi T, Kasal DA, Li MW, Shbat L, Laurant P, Neves MF, Paradis P, Schiffrin EL.** 2011. T regulatory lymphocytes prevent angiotensin II-induced hypertension and vascular injury. Hypertension **57:**469–476. http://dx.doi.org/10.1161/HYPERTENSIONAHA.110.162941.
11. **Kasal DA, Barhoumi T, Li MW, Yamamoto N, Zdanovich E, Rehman A, Neves MF, Laurant P, Paradis P, Schiffrin EL.** 2012. T regulatory lymphocytes prevent aldosterone-induced vascular injury. Hypertension **59:**324–330. http://dx.doi.org/10.1161/HYPERTENSIONAHA.111.181123.
12. **Muller DN, Shagdarsuren E, Park JK, Dechend R, Mervaala E, Hampich F, Fiebeler A, Ju X, Finckenberg P, Theuer J, Viedt C, Kreuzer J, Heidecke H, Haller H, Zenke M, Luft FC.** 2002. Immunosuppressive treatment protects against angiotensin II-induced renal damage. Am J Pathol **161:**1679–1693. http://dx.doi.org/10.1016/S0002-9440(10)64445-8.
13. **Crowley SD, Frey CW, Gould SK, Griffiths R, Ruiz P, Burchette JL, Howell DN, Makhanova N, Yan M, Kim HS, Tharaux PL, Coffman TM.** 2008. Stimulation of lymphocyte responses by angiotensin II promotes kidney injury in hypertension. Am J Physiol Renal Physiol **295:**F515–F524. http://dx.doi.org/10.1152/ajprenal.00527.2007.
14. **Mervaala E, Muller DN, Park JK, Dechend R, Schmidt F, Fiebeler A, Bieringer M, Breu V, Ganten D, Haller H, Luft FC.** 2000. Cyclosporin A protects against angiotensin II-induced end-organ damage in double transgenic rats harboring human renin and angiotensinogen genes. Hypertension **35:**360–366. http://dx.doi.org/10.1161/01.HYP.35.1.360.
15. **Guzik TJ, Hoch NE, Brown KA, McCann LA, Rahman A, Dikalov S, Goronzy J, Weyand C, Harrison DG.** 2007. Role of the T cell in the genesis of angiotensin II induced hypertension and vascular dysfunction. J Exp Med **204:**2449–2460. http://dx.doi.org/10.1084/jem.20070657.
16. **Madhur MS, Lob HE, McCann LA, Iwakura Y, Blinder Y, Guzik TJ, Harrison DG.** 2010. Interleukin 17 promotes angiotensin II-induced hypertension and vascular dysfunction. Hypertension **55:**500–507. http://dx.doi.org/10.1161/HYPERTENSIONAHA.109.145094.
17. **Shao J, Nangaku M, Miyata T, Inagi R, Yamada K, Kurokawa K, Fujita T.** 2003. Imbalance of T-cell subsets in angiotensin II-infused hypertensive rats with kidney injury. Hypertension **42:**31–38. http://dx.doi.org/10.1161/01.HYP.0000075082.06183.4E.
18. **Crowley SD, Song YS, Lin EE, Griffiths R, Kim HS, Ruiz P.** 2010. Lymphocyte responses exacerbate angiotensin II-dependent hypertension. Am J Physiol Regul Integr Comp Physiol **298:**R1089–R1097. http://dx.doi.org/10.1152/ajpregu.00373.2009.
19. **Harrison DG, Guzik TJ, Lob HE, Madhur MS, Marvar PJ, Thabet SR, Vinh A, Weyand CM.** 2011. Inflammation, immunity, and hypertension. Hypertension **57:**132–140. http://dx.doi.org/10.1161/HYPERTENSIONAHA.110.163576.
20. **Rodríguez-Iturbe B, Pons H, Herrera-Acosta J, Johnson RJ.** 2001. Role of immunocompetent cells in nonimmune renal diseases. Kidney Int **59:**1626–1640. http://dx.doi.org/10.1046/j.1523-1755.2001.0590051626.x.
21. **Rodríguez-Iturbe B, Pons H, Quiroz Y, Gordon K, Rincon J, Chavez M, Parra G, Herrera-Acosta J, Gomez-Garre D, Largo R, Egido J, Johnson RJ.** 2001. Mycophenolate mofetil prevents salt-sensitive hypertension resulting from angiotensin II exposure. Kidney Int **59:**2222–2232. http://dx.doi.org/10.1046/j.1523-1755.2001.00737.x.
22. **McMaster WG, Kirabo A, Madhur MS, Harrison DG.** 2015. Inflammation, immunity, and hypertensive end-organ damage. Circ Res **116:**1022–1033. http://dx.doi.org/10.1161/CIRCRESAHA.116.303697.
23. **Bustelo XR.** 2000. Regulatory and signaling properties of the Vav family. Mol Cell Biol **20:**1461–1477. http://dx.doi.org/10.1128/MCB.20.5.1461-1477.2000.
24. **Bustelo XR.** 2014. Vav family exchange factors: an integrated regulatory and functional view. Small GTPases **5**(2)**:**9. http://dx.doi.org/10.4161/21541248.2014.973757.
25. **Turner M, Billadeau DD.** 2002. VAV proteins as signal integrators for multi-subunit immune-recognition receptors. Nat Rev Immunol **2:**476–486. http://dx.doi.org/10.1038/nri840.
26. **Tarakhovsky A, Turner M, Schaal S, Mee PJ, Duddy LP, Rajewsky K, Tybulewicz VL.** 1995. Defective antigen receptor-mediated proliferation of B and T cells in the absence of Vav. Nature **374:**467–470. http://dx.doi.org/10.1038/374467a0.
27. **Turner M, Mee PJ, Walters AE, Quinn ME, Mellor AL, Zamoyska R, Tybulewicz VL.** 1997. A requirement for the Rho-family GTP exchange factor Vav in positive and negative selection of thymocytes. Immunity **7:**451–460. http://dx.doi.org/10.1016/S1074-7613(00)80367-2.
28. **Fujikawa K, Miletic AV, Alt FW, Faccio R, Brown T, Hoog J, Fredericks J, Nishi S, Mildiner S, Moores SL, Brugge J, Rosen FS, Swat W.** 2003. Vav1/2/3-null mice define an essential role for Vav family proteins in lymphocyte development and activation but a differential requirement in MAPK signaling in T and B cells. J Exp Med **198:**1595–1608. http://dx.doi.org/10.1084/jem.20030874.
29. **Sauzeau V, Sevilla MA, Rivas-Elena JV, de Alava E, Montero MJ, Lopez-Novoa JM, Bustelo XR.** 2006. Vav3 proto-oncogene deficiency leads to sympathetic hyperactivity and cardiovascular dysfunction. Nat Med **12:**841–845. http://dx.doi.org/10.1038/nm1426.
30. **Sauzeau V, Jerkic M, Lopez-Novoa JM, Bustelo XR.** 2007. Loss of Vav2 proto-oncogene causes tachycardia and cardiovascular disease in mice. Mol Biol Cell **18:**943–952. http://dx.doi.org/10.1091/mbc.E06-09-0877.
31. **Sauzeau V, Horta-Junior JAC, Riolobos AS, Fernandez G, Sevilla MA, Lopez DE, Montero MJ, Rico B, Bustelo XR.** 2010. Vav3 is involved in GABAergic axon guidance events important for the proper function of brainstem neurons controlling cardiovascular, respiratory, and renal parameters. Mol Biol Cell **21:**4251–4263. http://dx.doi.org/10.1091/mbc.E10-07-0639.
32. **Sauzeau V, Sevilla MA, Montero MJ, Bustelo XR.** 2010. The Rho/Rac exchange factor Vav2 controls nitric oxide-dependent responses in mouse vascular smooth muscle cells. J Clin Invest **120:**315–330. http://dx.doi.org/10.1172/JCI38356.
33. **Jonsson CA, Svensson L, Carlsten H.** 1999. Beneficial effect of the inosine monophosphate dehydrogenase inhibitor mycophenolate mofetil on survival and severity of glomerulonephritis in systemic lupus erythematosus (SLE)-prone MRL*lpr*/*lpr* mice. Clin Exp Immunol **116:**534–541. http://dx.doi.org/10.1046/j.1365-2249.1999.00901.x.
34. **Kassan M, Montero MJ, Sevilla MA.** 2010. In vitro antioxidant activity of pravastatin provides vascular protection. Eur J Pharmacol **630:**107–111. http://dx.doi.org/10.1016/j.ejphar.2009.12.037.
35. **Menacho-Márquez M, Garcia-Escudero R, Ojeda V, Abad A, Delgado P, Costa C, Ruiz S, Alarcon B, Paramio JM, Bustelo XR.** 2013. The Rho exchange factors Vav2 and Vav3 favor skin tumor initiation and promotion by engaging extracellular signaling loops. PLoS Biol **11:**e1001615. http://dx.doi.org/10.1371/journal.pbio.1001615.
36. **Paragas N, Qiu A, Hollmen M, Nickolas TL, Devarajan P, Barasch J.** 2012. NGAL-Siderocalin in kidney disease. Biochim Biophys Acta **1823:**1451–1458. http://dx.doi.org/10.1016/j.bbamcr.2012.06.014.
37. **Benigni A, Cassis P, Remuzzi G.** 2010. Angiotensin II revisited: new roles in inflammation, immunology and aging. EMBO Mol Med **2:**247–257. http://dx.doi.org/10.1002/emmm.201000080.
38. **Rees DD, Palmer RM, Hodson HF, Moncada S.** 1989. A specific inhibitor of nitric oxide formation from L-arginine attenuates endothelium-dependent relaxation. Br J Pharmacol **96:**418–424. http://dx.doi.org/10.1111/j.1476-5381.1989.tb11833.x.
39. **Sintchak MD, Nimmesgern E.** 2000. The structure of inosine 5′-monophosphate dehydrogenase and the design of novel inhibitors. Immunopharmacology **47:**163–184. http://dx.doi.org/10.1016/S0162-3109(00)00193-4.
40. **D'Alessio FR, Tsushima K, Aggarwal NR, West EE, Willett MH, Britos MF, Pipeling MR, Brower RG, Tuder RM, McDyer JF, King LS.** 2009. $CD4^+$ $CD25^+$ $Foxp3^+$ Tregs resolve experimental lung injury in mice and are present in humans with acute lung injury. J Clin Invest **119:**2898–2913. http://dx.doi.org/10.1172/JCI36498.
41. **Lewkowicz P, Lewkowicz N, Sasiak A, Tchorzewski H.** 2006. Lipopolysaccharide-activated $CD4^+$ $CD25^+$ T regulatory cells inhibit neutrophil function and promote their apoptosis and death. J Immunol **177:**7155–7163. http://dx.doi.org/10.4049/jimmunol.177.10.7155.

42. **Junger WG.** 2011. Immune cell regulation by autocrine purinergic signalling. Nat Rev Immunol **11:**201–212. http://dx.doi.org/10.1038/nri2938.
43. **Noris M, Casiraghi F, Todeschini M, Cravedi P, Cugini D, Monteferrante G, Aiello S, Cassis L, Gotti E, Gaspari F, Cattaneo D, Perico N, Remuzzi G.** 2007. Regulatory T cells and T cell depletion: role of immunosuppressive drugs. J Am Soc Nephrol **18:**1007–1018. http://dx.doi.org/10.1681/ASN.2006101143.
44. **Barrat FJ, Cua DJ, Boonstra A, Richards DF, Crain C, Savelkoul HF, de Waal-Malefyt R, Coffman RL, Hawrylowicz CM, O'Garra A.** 2002. In vitro generation of interleukin 10-producing regulatory $CD4^+$ T cells is induced by immunosuppressive drugs and inhibited by T helper type 1 (Th1)- and Th2-inducing cytokines. J Exp Med **195:**603–616. http://dx.doi.org/10.1084/jem.20011629.
45. **Hafiz MM, Faradji RN, Froud T, Pileggi A, Baidal DA, Cure P, Ponte G, Poggioli R, Cornejo A, Messinger S, Ricordi C, Alejandro R.** 2005. Immunosuppression and procedure-related complications in 26 patients with type 1 diabetes mellitus receiving allogeneic islet cell transplantation. Transplantation **80:**1718–1728. http://dx.doi.org/10.1097/01.tp.0000187881.97068.77.
46. **Banerjee R, Halil O, Bain BJ, Cummins D, Banner NR.** 2000. Neutrophil dysplasia caused by mycophenolate mofetil. Transplantation **70:**1608–1610. http://dx.doi.org/10.1097/00007890-200012150-00012.
47. **Nogueras F, Espinosa MD, Mansilla A, Torres JT, Cabrera MA, Martin-Vivaldi R.** 2005. Mycophenolate mofetil-induced neutropenia in liver transplantation. Transplant Proc **37:**1509–1511. http://dx.doi.org/10.1016/j.transproceed.2005.02.038.
48. **Cowley AW, Jr.** 1992. Long-term control of arterial blood pressure. Physiol Rev **72:**231–300.
49. **Hwang S, Song KD, Lesourne R, Lee J, Pinkhasov J, Li L, El-Khoury D, Love PE.** 2012. Reduced TCR signaling potential impairs negative selection but does not result in autoimmune disease. J Exp Med **209:**1781–1795. http://dx.doi.org/10.1084/jem.20120058.
50. **Ruiz S, Santos E, Bustelo XR.** 2009. The use of knockout mice reveals a synergistic role of the Vav1 and Rasgrf2 gene deficiencies in lymphomagenesis and metastasis. PLoS One **4:**e8229. http://dx.doi.org/10.1371/journal.pone.0008229.
51. **Sommers CL, Lee J, Steiner KL, Gurson JM, Depersis CL, El-Khoury D, Fuller CL, Shores EW, Love PE, Samelson LE.** 2005. Mutation of the phospholipase C-γ1-binding site of LAT affects both positive and negative thymocyte selection. J Exp Med **201:**1125–1134. http://dx.doi.org/10.1084/jem.20041869.
52. **Sakaguchi N, Takahashi T, Hata H, Nomura T, Tagami T, Yamazaki S, Sakihama T, Matsutani T, Negishi I, Nakatsuru S, Sakaguchi S.** 2003. Altered thymic T-cell selection due to a mutation of the ZAP-70 gene causes autoimmune arthritis in mice. Nature **426:**454–460. http://dx.doi.org/10.1038/nature02119.
53. **Pan D, Amison RT, Riffo-Vasquez Y, Spina D, Cleary SJ, Wakelam MJ, Page CP, Pitchford SC, Welch HC.** 2015. P-Rex and Vav Rac-GEFs in platelets control leukocyte recruitment to sites of inflammation. Blood **125:**1146–1158. http://dx.doi.org/10.1182/blood-2014-07-591040.
54. **Lawson CD, Donald S, Anderson KE, Patton DT, Welch HC.** 2011. P-Rex1 and Vav1 cooperate in the regulation of formyl-methionyl-leucyl-phenylalanine-dependent neutrophil responses. J Immunol **186:**1467–1476. http://dx.doi.org/10.4049/jimmunol.1002738.